

Robotic technology and endoluminal surgery in digestive surgery

*Original*

Robotic technology and endoluminal surgery in digestive surgery / Volpato, Silvio. - (2018 Jun 15).  
[10.6092/polito/porto/2709912]

*Availability:*

This version is available at: 11583/2709912 since: 2018-06-21T20:28:59Z

*Publisher:*

Politecnico di Torino

*Published*

DOI:10.6092/polito/porto/2709912

*Terms of use:*

Altro tipo di accesso

This article is made available under terms and conditions as specified in the corresponding bibliographic description in the repository

*Publisher copyright*

(Article begins on next page)



**ScuDo**  
Scuola di Dottorato ~ Doctoral School  
WHAT YOU ARE, TAKES YOU FAR

Doctoral Dissertation  
Doctoral Program in Bioengineering and Medical-Surgical Sciences (30<sup>th</sup> Cycle)

# **Robotic technology and endoluminal surgery in digestive surgery**

By

**Silvio Volpato**

\*\*\*\*\*

**Supervisors:**

Prof. Mario Morino, Supervisor  
Prof. Alberto Arezzo, Co-Supervisor

**Doctoral Examination Committee:**

Prof. Luigi Boni, Referee, University of Milano  
Prof. Nicola Di Lorenzo, Referee, University of Tor Vergata, Roma  
Prof. Giuseppe Galloro, Referee, University Federico II, Napoli  
Prof. Sergio Gentili, Referee, University of Eastern Piedmont

Politecnico di Torino  
2017

## **Declaration**

I hereby declare that, the contents and organization of this dissertation constitute my own original work and does not compromise in any way the rights of third parties, including those relating to the security of personal data.

Silvio Volpatto

2017

\* This dissertation is presented in partial fulfillment of the requirements for **Ph.D. degree** in the Graduate School of Politecnico di Torino (ScuDo).

*I would like to dedicate this thesis to Loredana and Laura*



## **Acknowledgment**

And I would like to acknowledge for her help Margherita Brancadoro, MSc, BSc Biomedical Engineer, at The BioRobotics Institute, Scuola Superiore Sant'Anna, Polo Sant'Anna Valdera, Pontedera (Pisa), Italy.

## Abstract

**Background.** Colorectal cancer (CRC) is the third most common cancer in males and second in females, and the fourth most common cause of cancer death worldwide. The implementation of screening programs has allowed to the identification of an increasing number of early-stage neoplastic lesions. Presently, superficial colorectal neoplasms (including precancerous lesions and early cancer) can be resected in the colon by Endoscopic Mucosal Resection (EMR) and Endoscopic Submucosal Dissection (ESD), while in the rectum by Transanal Endoscopic Microsurgery (TEM). They are the preferred choices inside of the minimally invasive panorama regarding the CRC treatment. TEM technique offers more advantages than EMR and ESD, but it can't overcome the recto-sigmoid junction. Many authors, research institutes and biomedical industries have proposed different solutions for microsurgery dissection of early lesions in the colon, but all these proposals have in common the development of platforms expressly designed for this use, with significant purchasing and management costs. The aim of our research project is to develop a robotic platform that allows to treat lesions throughout the colon limiting the costs of management and purchasing. This new robotic platform, developed in collaboration with Scuola Superiore Sant'Anna in Pisa, is called RED (Robot for Endoscopic Dissection). At the tip of a standard endoscope a hood (RED) is placed. RED is equipped by two extractable teleoperated robotic arms (*i.e.*, diathermic hook and gripper); their motion is provided by onboard miniaturized commercial motors and a dedicated external platform. The endoscopist holds the endoscope near the lesion, while the operator drives the robotic arms through a remote control.

**Materials and Methods.** Several preliminary studies have been conducted in the following order. A first test was conducted for identification of force value for lifting and pulling maneuvers using a modified TEM instrument. A CAD study was conducted to determine the maximum size that the hood must have in order to overcome the critical angle represented by the splenic flexure. Several tests were

conducted to determine the degrees of freedom of each robotic arm, starting with the CAD drawing to make subsequently the mock-ups of each configuration. Finally, a 3D mock-up was produced that was assembled on an endoscope to perform the in vitro test to evaluate the workspace and field of view using a pelvic trainer for TEM.

**Results.** The first test shown that the minimum force that the gripper will have to develop with the push-pull is 1.5N. The CAD study shown that the maximum dimensions the hood must have to overcome splenic flexure are: maximum diameter 28mm, maximum length 57mm. After several configurations was been tested, the final prototype features are: gripper arm with pitch sliding and open/close of the tip and diathermic hook arm with pitch, roll and sliding. There will be 6 such distributed motors: 3 external motors for the gripper arm that will operate through cables contained in a sheath adherent to colonoscope and 3 embedded motors for diathermic hook arm (one integrated on the hood for the sliding degree of motion and the other two inside of the arm). The in-vitro test has been carried out to evaluate the workspace and they proved that the operating field vision is not obstructed by the hood and the working range is sufficiently wide to perform a dissection.

**Conclusion.** Tests conducted up to this point have allowed us to identify the overall layout of the RED: dimensions, degrees of freedom, number and distribution of motors needed for the operation of robotic arms; moreover, it is proved that the device, once assembled, maintained the visual and operational field characteristics necessary to perform an accurate dissection. The next step will be to realize a RED steel final prototype and in-vivo tests will be carry out to replicate an endoscopic dissection into the colon.



# Index

1. Early stage colorectal cancer: problems and state of the art.....	1
1.1 Introduction .....	1
1.2 Early stage colorectal cancer standard treatment .....	2
1.2.1 Endoscopic Mucosal resection (EMR) .....	2
1.2.2 Endoscopic Submucosal Dissection (ESD) .....	2
1.2.3 Transanal Endoscopic Microsurgery (TEM) .....	3
1.3 Surgical instruments with robotic arms .....	5
1.3.1 Endoscopic platform .....	5
1.3.2 Research device.....	13
1.3.3 Research platform and articulated robots.....	17
2. RED: a new endoscopic robotic platform.....	27
2.1 Aim of the research.....	27
2.1 Research overview.....	28
3. Materials and Methods.....	30
3.1 Identification of force value .....	30
3.2 Estimate of maximum external size of the device.....	33
3.3 Assessment of the overall dimension: in vitro tests and mock-up creations .....	35
4. Results.....	43
4.1 Identification of force value .....	43
4.2 Estimate of maximum external size of the device.....	43

4.3 Assessment of the overall dimension: in vitro tests and mock-up creations .....	45
4.3.1 Flexibility test with hood .....	45
4.3.2 Workspace definition tests .....	46
4.3.2.1 DoF of gripper robotic arm.....	46
4.3.2.2 DoF of diathermic hook robotic arm .....	47
4.3.2.3 RED final design and in-vitro test for workspace assessment...	49
5. Discussion.....	55
6. Conclusion .....	59
7. References.....	60



# List of Figures

Figure 1: EMR procedure.....	2
Figure 2: ESD procedure.....	3
Figure 3: TEM procedure.....	4
Figure 4: Dissection with TEM.....	5
Figure 5: Specifications of the USGI Transport scope .....	6
Figure 6: Cobra system .....	6
Figure 7: R-Scope system .....	7
Figure 8: Endosamurai system.....	8
Figure 9: Neo-Guide Endoscopy System.....	9
Figure 10: The STRAS system is a robotized version of the Anubiscope.....	9
Figure 11: The Direct Drive Endoscopic System.....	10
Figure 12: Spider system.....	11
Figure 13: The Via-Cath endoluminal system .....	11
Figure 14: Endomina system.....	12
Figure 15: Instrument field of action in various systems when endoscope movement is excluded.....	13
Figure 16: MASTER system.....	14
Figure 17: Image and main features of telemanipulated system presented by de Mathelin et al.....	15
Figure 18: Scheme of HVSPS system.....	15
Figure 19: HVSPS system.....	16
Figure 20: Master–slave robotic system introduced by Fujie et al. ....	16
Figure 21: System develop by Imperial College of London .....	17
Figure 22: Flex robotic system.....	17
Figure 23: I-snake system overview.....	18
Figure 24: IREP system.....	19



Figure 25: System developed by Yang et al.....	19
Figure 26: Scheme of first prototype of the system presented by Phee et al. ....	20
Figure 27: Kinematic of SPRINT robotic arm.....	20
Figure 28: The Dexterous in vivo robot system developed by Lehman .....	21
Figure 29: Miniature in vivo robotic platform for LESS setup in operative room.....	21
Figure 30: Miniature in vivo robotic platform for LESS robotic arms.....	22
Figure 31: DoF of robotic arms and remote control.....	23
Figure 32: Single-port surgery robotic system developed by Kobayashi et al. ....	24
Figure 33: Virtual Incision.....	24
Figure 34: da Vinci Surgical System (Intuitive Surgical).....	25
Figure 35: The SurgiBot System (TransEnterix) .....	25
Figure 36: SPORT Surgical System (Titan Medical Inc.) .....	26
Figure 37: RED in operative position .....	29
Figure 38: Rendering of the operative room .....	29
Figure 39: Lifting and pulling force during dissection .....	30
Figure 40: Scheme of force measurement system.....	31
Figure 41: a) Scheme for the measurement setup. b) Corresponding involved forces; $F_r$ , $F_s$ , $F_t$ can be along $\pm z$ or $\pm x$ .....	33
Figure 42: Schematic representation on colonic segment.....	34
Figure 43: Example of Data Card for Olympus GIF-HQ190 Gastroscope.....	35
Figure 44: The darkest point at the tip represents the rigid and non-flexible endoscope cap. The yellow cone is instead the field of vision. ....	36
Figure 45: Cylindrical cap representing RED .....	37
Figure 46: Scheme of 4 DoF robotic arms .....	38
Figure 47: CAD assembling with 4 DoF.....	39
Figure 48: Mock-up assembling of robotic arm with 4 DoF.....	39
Figure 49: Scheme of 2 DoF placed at the base of robotic arm .....	39

Figure 50: CAD assembly .....	40
Figure 51: Scheme of 2 DoF with roll at the tip of robotic arm.....	40
Figure 52: CAD and Mock-up assembly of 2 DoF robotic arm with roll at the tip .....	41
Figure 53: 1 DoF robotic arm.....	41
Figure 54: CAD design of 1 DoF robotic arm .....	42
Figure 55: angles position of diathermic hook.....	42
Figure 56: CAD design of splenic flexure. The red rectangle represents the maximum size that allows to cross the flexure. ....	44
Figure 57: Flexibility test with cap 26mm diameter and 50mm length .....	45
Figure 58: Representing degrees of freedom, CAD design and mock-up of gripper robotic arm .....	46
Figure 59: Classic laparoscopic fenestrate gripper .....	47
Figure 60: Representing degrees of freedom, CAD design and mock-up of diathermic hook robotic arm.....	47
Figure 61: First mock-up assembly .....	48
Figure 62: Scheme of gripper arm with pitch at the base and sliding (green arrows) .....	49
Figure 63: CAD design of gripper arm .....	49
Figure 64: CAD design of gripper movement.....	50
Figure 65: CAD design of the plastic gripper hood .....	50
Figure 66: Diathermic hook arm .....	51
Figure 67: Internal view of diathermic hook arm with the position of the two motors .....	51
Figure 68: CAD design of the hood .....	52
Figure 69: Definitive mock-ups. A) Gripper. B) Diathermic hook. C) Hood.	53
Figure 70: RED assembled and installed on an endoscope.....	53
Figure 71: RED operative vision.....	54

## List of Tables

Table 1: Summary of mechanical and robotic flexible endoscopic multitasking platform.....	12
Table 2: Comparison of the colonic segmental diameter .....	34
Table 3: Comparison of the colonic segmental angle .....	34
Table 4: Summary of the forces measured in the in-vivo and ex-vivo tests ...	43



# **Chapter 1**

## **Early stage colorectal cancer: problems and state of the art**

### **1.1 Introduction**

Colorectal cancer (CRC) is the third most common cancer in males and second in females, and the fourth most common cause of cancer death worldwide. Currently, about 60-70% of diagnosed cases in symptomatic patients are detected at an advanced stage of disease. Earlier stage detection using screening strategies allow better outcomes, both as much survival rates than in terms of reducing the disease burden for Public Health (1).

Colonoscopy is a widely-accepted method for detecting and treating CRC at an early stage to decrease CRC incidence and mortality. Presently, superficial colorectal neoplasms, including precancerous lesions and early cancer, can be detected and evaluated by white light endoscopy, chromo-endoscopy and magnifying endoscopy, and be resected in the colon by Endoscopic Mucosal Resection (EMR) and Endoscopic Submucosal Dissection (ESD), which in the rectum by Transanal Endoscopic Microsurgery (TEM), all minimally invasive technique, and have become the preferred choices (2).

## 1.2 Early stage colorectal cancer standard treatment

The following sections shortly present the main endoscopic surgical techniques used to treat early stage CRC lesions.

### 1.2.1 Endoscopic Mucosal resection (EMR)

EMR is a technique used for the staging and treatment of superficial neoplasms of the GI tract (3). EMR consists on the removal of injury tissue through diathermy loop that is introduced through the operative channel of the flexible endoscope and upon lifting of the lesion through the infiltration of a saline solution in the submucosal layer of the wall (Figure 1).

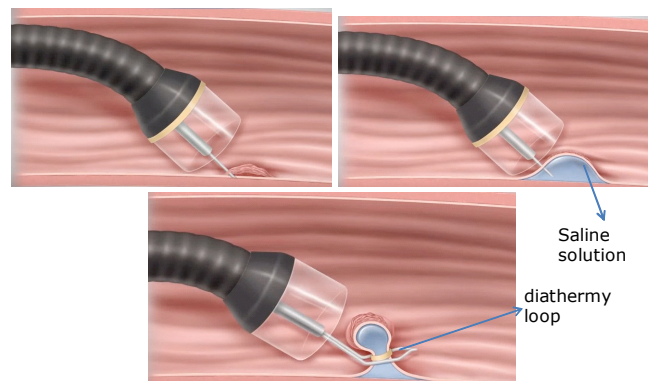


**Figure 1:** EMR procedure

Although EMR are safe, convenient, and efficacious, they are unsuitable for large lesions in particular. Difficulty in correctly assessing the depth of tumor invasion and an increase in local recurrence when standard EMR procedures are used have been reported in cases of large lesions, because such lesions are often resected piecemeal owing to the technical limitations of standard EMR (4). This method makes it possible for there to be an en-bloc excision only for lesions with dimensions that are up to 2 cm and it carries the burden of a high rate of local relapse.

### 1.2.2 Endoscopic Submucosal Dissection (ESD)

An alternative method is represented by the ESD (5). This technique, initially developed to treat early gastric cancer, allows the direct dissection of the

submucosa, and large lesions can be resected en-bloc; it is again carried out by means of a flexible endoscope introducing special diathermic dissector scalpel through the operating channel. At present, numerous electrosurgical knives such as insulation-tipped diathermic knife (IT-knife), needle knife, hook knife, flex knife, triangle-tipped knife, flush knife, mucosectomy, splash needle and a special device called a small-caliber tip transparent (ST) hood are available for this technique (Figure 2).

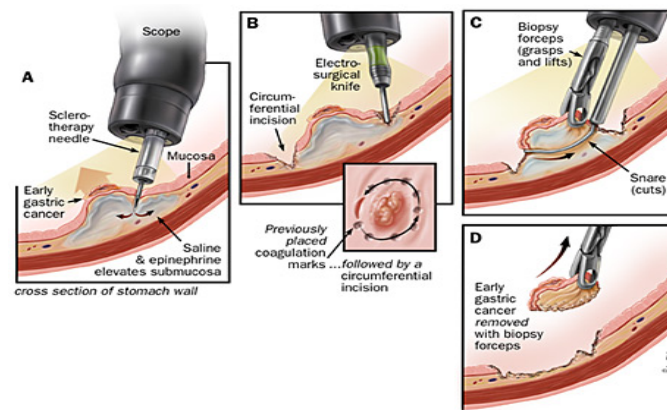


**Figure 2:** ESD procedure

However, ESD is associated with high risks of complications and the procedures are long, often requiring more than 90min for lesions of even only 3-4cm in diameter. The risk of haemorrhage ranges from 3.5% to 15.5% and the possibility of intestinal perforation is also high (up to 18%) (6). Furthermore, the percentage of en-bloc excision that goes from 50 to 80% for lesions wider than 2 cm, according to the published experiences.

### 1.2.3 Transanal Endoscopic Microsurgery (TEM)

The TEM procedure (Figure 3), originally developed by G.F. Buess, has been suggested as a novel alternative approach for the local excision of rectal neoplasms, especially those located in the middle and upper rectum. The available reports on TEM excision of rectal tumors have suggested that the described procedure is a safe and efficient technique for the removal of rectal tumors (7).

This minimally invasive technique offers the advantages of superior visualization of the lesion and greater access to proximal lesions with lower

margin positivity and specimen fragmentation and lower long-term recurrence rates over traditional transanal excision (6).

Standard TEM instruments include a 40mm diameter operating rectoscope in 70mm, 120mm and 200mm lengths, with bevelled tips. Today, the most used platform is the TEO (Karl Storz, Tuttlingen, Germany), which is provided in two different lengths of 75mm and 150mm, but with the same 40mm diameter. The rectoscope is connected to a dedicated plate that incorporates a microscope-laparoscope aperture and a large opening with silastic seals for rigid instruments.

A 5mm 30° optics and three rigid 5mm instruments are introduced through these dedicated ports on the front of the rectoscope (Figure 3).

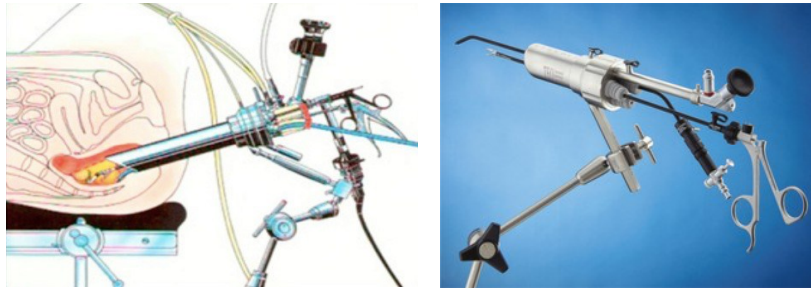


**Figure 3:** TEM procedure

One instrument is used for grasping the lesion and exposing it, and another is used for cutting the tissue with a high frequency dissector. The dissection is performed circumferentially around the lesion. The exposure of the tissue consists of a lifting and pulling of the tissue in order to put sufficient tension on it, which allows easier dissection (Figure 4).



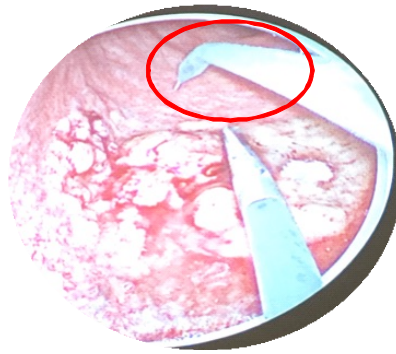


**Figure 4:** Dissection with TEM

### 1.3 Surgical instruments with robotic arms

This part is an overview of different robotic platforms for flexible access surgery (8-35).

#### 1.3.1 Endoscopic platform

- **Trasport** (USGI Medical, San Clemente, CA, USA) utilizes the stiffening endoscopic over-tube technology named Shape-lock. The system also incorporates four large working ports (7, 6, 4 and 4mm), an insufflation channel and four-direction flexibility at the tip. A standard flexible endoscope can be passed through the 6mm port. Although better than the traditional endoscope, triangulation is still relatively poor. Furthermore, the device is quite complex to manipulate and a significant learning curve is associated with its use. Finally, smooth and precise motion of the tip, and therefore of the surgical tools, is difficult (Figure 5).



Outside diameter	18 mm
Number of instrument channels	4
Instrument channel size	7 mm, 6 mm, 4 mm, 4 mm
Length	110 cm

**Figure 5:** Specifications of the USGI Transport scope

- **Cobra** (USGI Medical, San Clemente, CA, USA): it solves the problem of triangulation by adding three independent arms to the Shape-lock©-based shaft of the Transport (Figure 6). Currently the controls are tendon-driven and inaccurate, making it difficult to perform fine movements. Another limitation is that the device must be removed to exchange instruments and then reintroduced because the tools are fixed.



**Figure 6:** Cobra system

- **Incision Operating Platform** (USGI Medical, San Clemente, CA, USA): The design of this is based on the Transport, but with the integration of an ergonomic user interface to improve bimanual coordination.
- **R-Scope** (Olympus, Tokyo, Japan): adapted a standard dual channel scope in order to make it functional for advanced endoluminal operation, the R-scope has an outside diameter of 14.3mm and a length of 103mm, while each instrument channel has a size of 2.8mm and elevators allowing independent motion of tools in perpendicular planes (Figure 7). This permits dynamic retraction and cutting independent of the optical axis. Finally, a larger, separate channel for suction and irrigation is also incorporated.



**Figure 7:** R-Scope system

- **EndoSamurai** (Olympus, Tokyo, Japan): is based on the R-scope concept. A standard stereo endoscope's tip is fitted with two bendable hollow arms, giving two extra degrees of freedom (DoF) to operate the passive instruments inserted through them (Figure 8).



**Figure 8:** Endosamurai system

- **Neo-Guide Endoscopy System (NES)** (NeoGuide System Inc., now acquired by Intuitive Surgical Inc.): consists of a navigation console and a flexible endoscope with an embedded position sensor at the tip to measure the endoscopist steering commands and an external position sensor at the base which measures its insertion depth. It consists of a 173cm-long endoscope composed of sixteen 8cm-long independent vertebrae (Figure 9). Each segment can be directed to assume a right, left, up, down, circular curve, or a combination of these motions. During manual insertion of the device, the position and angle of the scope tip are encoded into a computer algorithm. As the colonoscope is advanced, the computer directs each successive vertebra to take the same shape that the tip had at a given insertion depth. The insertion tube thus changes its shape at different insertion depths in a “follow-the-leader” manner. The cross-sectional diameter of the NeoGuide™ insertion tube is approximately 14mm at the tip, increasing to approximately 20mm at the proximal shaft of the scope (the working channel is 3.2mm). The mechanical valves that control insufflation, suction, or water irrigation are the same as in conventional endoscopes. Biopsies and therapeutic maneuvers are

conducted with the scope in passive mode; where the shape and stiffness of the endoscope is the same as that of a standard colonoscope (9).

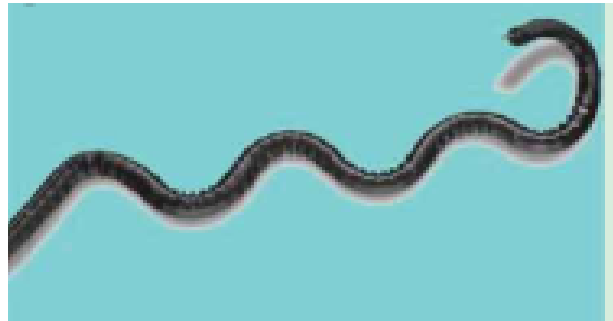


**Figure 9:** Neo-Guide Endoscopy System

- **Anubiscope** (Karl Storz Endoskope, Tuttlingen, Germany): It consists of a multifunctional endoscope with a diameter of 16mm and a tulip-shaped distal tip (Figure 10). When the operative site is reached, the flaps open to reveal two triangulating movable arms with working channels for flexible instrument insertion (24).



**Figure 10:** The STRAS system is a robotized version of the Anubiscope.

- **The Direct Drive Endoscopic System (DDES)** (Boston Scientific, Natick, MA, USA): It features a rail platform that can be attached directly to the operating table in an optimal ergonomic configuration and houses two handles to operate specifically designed long flexible instruments with different end-effectors (Figure 11). The instruments are inserted together with a standard endoscope through a flexible guide sheath that can be locked in any articulated configuration. This introduces two extra DoF for proximal positioning of the instruments, giving a total of 7 DoF.



**Figure 11:** The Direct Drive Endoscopic System

- **Spider** (TransEnterix Inc., Durham, NC, USA): The first generation of the system comprises an 18mm outer diameter delivery tube with four working channels. Two channels are rigid and can accommodate a standard endoscope or rigid laparoscopic instruments. The other two channels extend laterally to facilitate manipulation of flexible surgical instruments (Figure 12).

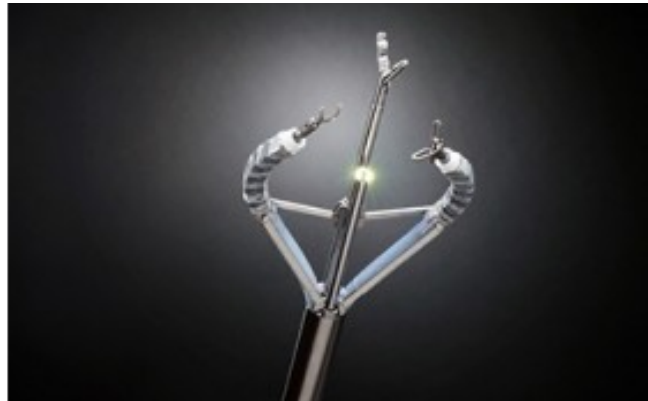


**Figure 12:** Spider system

- The **Via-Cath endoluminal system** (EndoVia Medical, now acquired by Hansen Medical, Norwood, MA, USA): is a flexible instrument with a diameter of 4.5mm. It has seven degrees of freedom controlled by 14 tension cables orientated in a special manner to allow instrument axial torque, axial loading and bending (Figure 13). The instrument has two distal multibending segments. It is capable of generating a tip force of up to 3N (9).



**Figure 13:** The Via-Cath endoluminal system

- **Endomina** (Endo Tools Therapeutics, a spin-off from the ULB), an innovative device that adds degrees of freedom and a number of therapeutic channels to existing endoscopes (Figure 14). It has two instrument channels with 3 DoF of independent movement. These channels are able to guide two

standard flexible instrument of up to 9 Fr in diameter. The system is actuated through electromechanically actuated traction cables. The control interface consists of two joysticks.

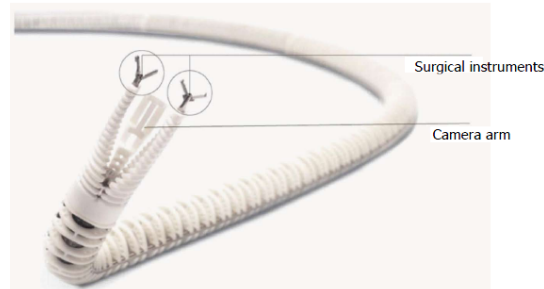


**Figure 14:** Endomina system

The Table 1 summarizes the main technical features while Figure 15 show field of action of every system above illustrated.

Name	Outer diameter (mm)	Number of instrument channels	Channel size (mm)	Length (cm)	Degree of freedom of movements	
Mechanical systems						
Integrated Mechanical Platforms						
Dual channel UGI Endoscope (Olympus, Japan)	12.6	2	3.7, 2.8	103	Endoscope Up/Down Left/Right Rotation Translation	Instrument Translation Open/Close
R-Scope (Olympus, Japan)	14.3	2	2.8 (deflectable)	133	Endoscope Up/down Left/right Rotation Translation	Instrument Translation Open/Close Up/Down Left/Right
EndoSamurai (Olympus, Japan)	15 (endoscope) 18 (over-tube)	3	2.8	103	Endoscope Up/down Left/right Rotation Translation	Instrument Up/Down Left/Right Translation Open/close Rotation
Anubis (KarlStorz, Germany)	16	3	4.2 * 2 (deflectable) 3.2 (central)	110	Endoscope Up/down Left/right Rotation Translation	Instrument Up/down Left/Right Open/close Translation Rotation
Platforms based on an access device						
Incisionless Operating Platform (USGI, USA)	18	4	7,6,4,4	110	Oversheath Up/down Left/right Rotation Translation	Instrument Up/down Left/right Open/dose Translation Rotation
DDES (Boston Scientific, USA)	16 * 22	3	7, 4.2, 4.2	55	Oversheath Up/down Left/right Rotation Translation	Instrument Up/down Left/right Open/dose Translation Rotation
Robotic systems						
MASTER (NanYang Tech Uni, Singapore)	22	Externally attached to endoscope 2 manipulator arms	—	150 cm (sheath) 41.7 mm (manipulator)	Endoscope Up/down Left/right Rotation Translation	Robotic arm Translation Elbow Flex/Ext Elbow Sup/Pron Wrist Flex/Ext Gripper Open/Close
ViaCath (Hansen medical, USA)	16	—	—	90	Instrument Up/Down/ Left/Right (in each of two distal segments) Translation Rotation Open/Close	

**Table 1:** Summary of mechanical and robotic flexible endoscopic multitasking platform



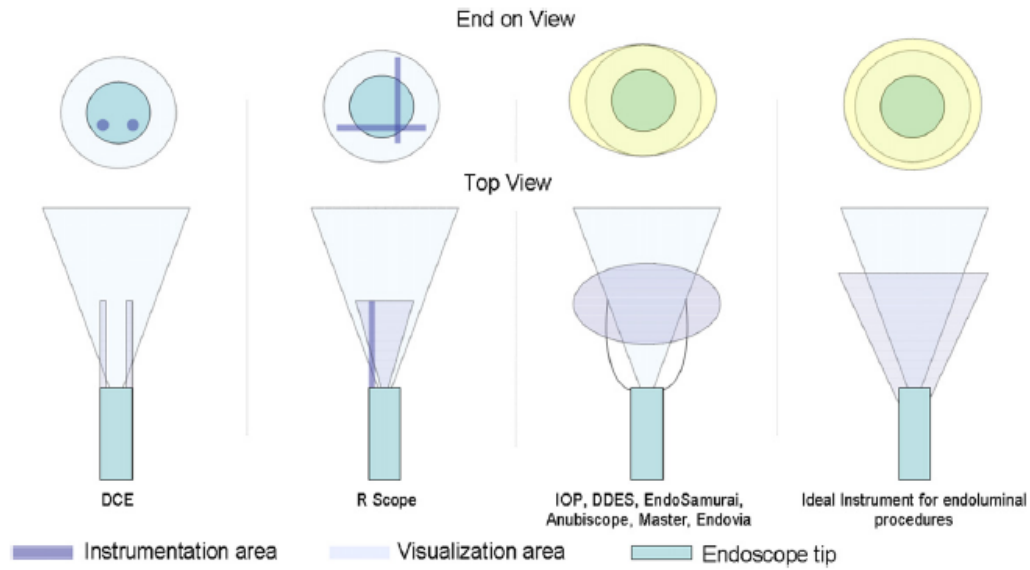


**Figure 15:** Instrument field of action in various systems when endoscope movement is excluded.

### 1.3.2 Research device

- The **Master And Slave Transluminal Endoscopic Robot (MASTER)** by Phee et al. (12,13). The system consists of a slave manipulator that can be attached to the tip of a standard dual-channel endoscope and features a translating DoF to sliding within its internal channels so that no external overtube is required. The two-armed robot has a total of 9 DoF (four for each arm plus one gripper), seven of which are remotely controlled using two handles and a foot pedal at the master console, while the translational ones are directly driven by the operator. The mechanical joints are tendon-actuated. The robotic arms extend up to 4cm out of the distal tip of the endoscope (Figure 16).

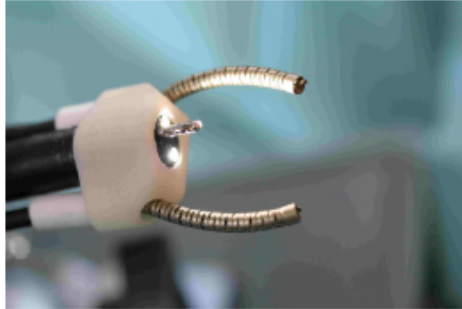
The system was operated by 2 operators, 1 responsible for the steering of the endoscope while the other responsible for performing the submucosal dissection with the 2 robotic arms.



**Figure 16:** MASTER system

- Another robotically telemanipulated system for transluminale surgery was presented by de Mathelin et al. (14,15). The slave part of the system is directly attached to the tip of a standard endoscope using a special cap and it consists of two snakelike hollow arms providing 2 DoF each to operate the instruments introduced through them. The endoscope provides the optical system for visual feedback and two working channels for conventional instruments. The hollow arms are fixed on the circumference at the end-part of the bending tip of the endoscope using a specific cap. Each arm provides 2 DOF similarly to the main endoscope: left/right and up/down motions. Surgical instruments can be introduced into the arms and guided to the operating area. These instruments can translate and rotate inside the arms (Figure 17).

The orientation of the main endoscope as well as the orientation of both arms is driven by two cables which run through the flexible shaft up to the proximal end where they are rolled up around pulleys.



	Max req. torque	motor	max. continuous mot. torque
Main endoscope	1.3Nm	HD FHA	1.5Nm
Hollow arms	0.20Nm	HD RSF	0.45Nm

**Figure 17:** Image and main features of telemanipulated system presented by de Mathelin et al.

- The **Highly Versatile Single Port System (HVSPS)** by Can et al. (16,31): The two flexible and partially automated manipulators are teleoperated using joysticks and feature 5 DoF. Triangulation is ensured by the use of a third arm to place a standard endoscope in an S-shape perpendicularly to the plane of the instruments. The manipulator has an outer diameter of 12mm (Figure 18, 19).

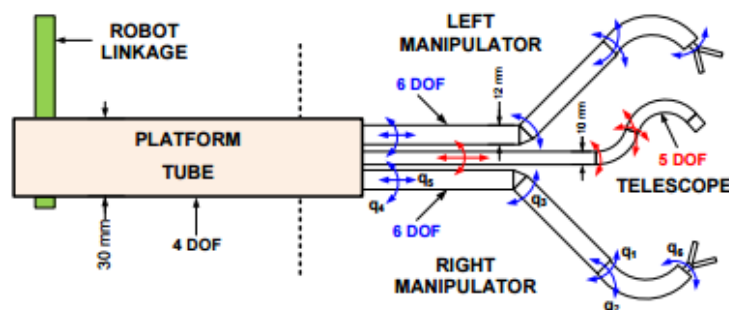


**Figure 18:** Scheme of HVSPS system



**Figure 19:** HVSPS system

- A recent master–slave robotic system for LESS was introduced by Fujie et al. (17). It features a slave part comprising a positioning manipulator which pivots a rigid insertable tool around the entry point at the skin incision. The distal end of the insertable tool is flexible and is connected to the rigid part through a 2 DoF snake-like continuum sheath manipulator. A flexible endoscope and two custom-made endoscopic tools are protruding from the distal tip in a configuration allowing triangulation. It has a diameter of 30mm (Figure 20).



**Figure 20:** Master–slave robotic system introduced by Fujie et al.

- The Imperial College of London (25) has also developed a robot prototype which has two instrument channels of 3mm and 2.5mm (Figure 21). Each

instrument channel has 3 DoF of movement. Each DoF of movement is controlled by two NiTi tendon. The platform's minimum overall diameter is 13mm.

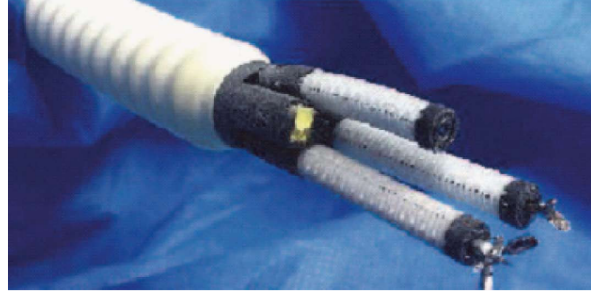


**Figure 21:** System develop by Imperial College of London

### 1.3.3 Research platform and articulated robots

- **Flex robotic system** (Medrobotics): The articulated part comprises two concentric tubes consisting of 50 cylindrical links connected in series through spherical joints, allowing 10 bending between adjacent links. Follow-the-leader motion is achieved by alternating the rigidity of the inner and outer tubes. Two inner channels allow for the passage of an endoscopic camera or instrumentation. It also integrates a stiffening overtube and two lateral flexible ports for the insertion of flexible instruments (Figure 22).



**Figure 22:** Flex robotic system

- **I-Snake** by Yang et al. (18). The main novelty of the device is the modular joint unit based on a hybrid micromotor/tendon design which allows independent control of each rotational DoF while leaving sufficient space for internal channels within the links. One channel is used to deploy a standard endoscopic camera, while the second channel enables the passage of various endoscopic instruments during the procedure. The enhanced dexterity of the device allowed complete retroflexion for stable tubal ligation (Figure 23).

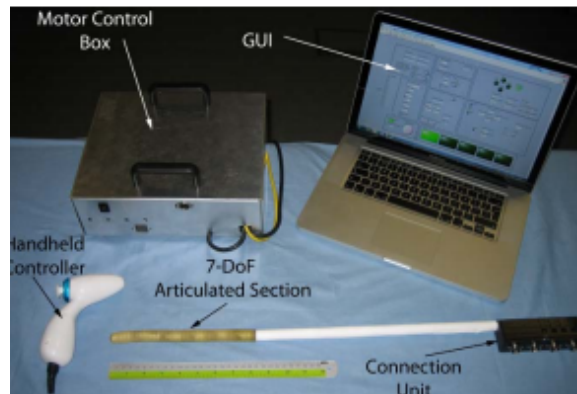


**Figure 23:** I-snake system overview

- **Insertable Robotic Effectors Platform (IREP)**, Simaan et al. (19) with integrated 3-D vision and surgical tools, which can be folded into a 15mm diameter configuration for deployment through a standard trocar port (Figure 24). The device uses 21 actuators to control gross translation movement along the IREP axis, the pan, tilt and zoom of the camera (3 DoF), two 2-DoF five-bar mechanisms to fold, unfold and regulate the distance between the flexible arms, and each dexterous arm featuring 6 DoF (a 4-DoF continuum snake-like robot, a 1-DoF wrist and a gripper).

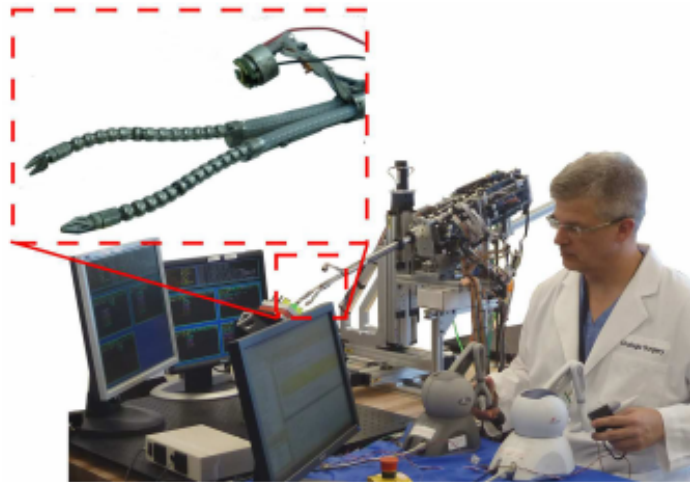


**Figure 24:** IREP system

- System developed by Yang et al. (20). The device comprises a proximal actuation pack, a rigid delivery shaft and a distal flexible unit. The latter is constituted of a 3-DoF articulated head mounted on a flexible tendon-driven neck (Figure 25).

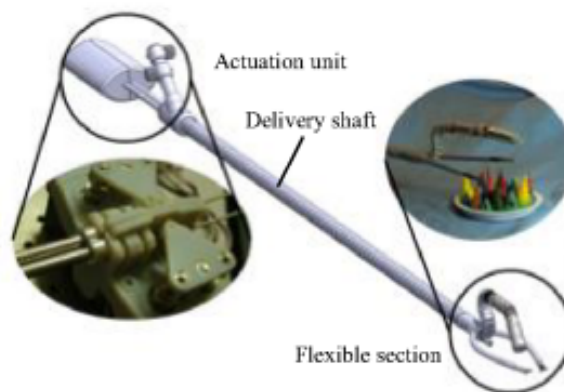


**Figure 25:** System developed by Yang et al.

- Phee et al. from Nanyang University have presented a master–slave robotic system designed for use with flexible endoscopy (Figure 26). The slave is a cable-driven flexible robotic manipulator that can be attached to an endoscope, allowing two-handed endoscopic manipulation with 9–12 DOF (35):



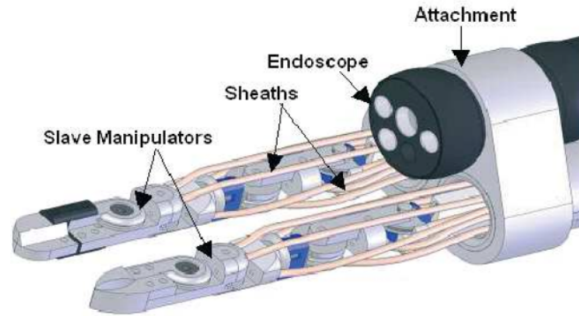


**Figure 26:** Scheme of first prototype of the system presented by Phee et al.

- **Single-Port laparoscopy bImaNual roboT (SPRINT)** consisting of two 6-DoF miniature arms that can be passed in turn through a 30mm trocar port at the umbilicus and then unfolded into a configuration similar to the one of the human arms (Figure 27).

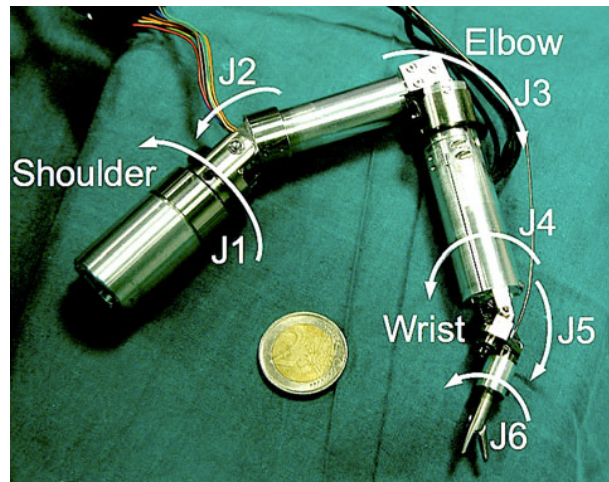


**Figure 27:** Kinematic of SPRINT robotic arm

- The **Dexterous in vivo robot system** has been developed by Lehman et al. from University of Nebraska (21). The robot features a central body carrying an on-board camera and magnets for magnetic external navigation, and two



foldable arms with cautery and forceps end-effectors to allow for flexible transgastric access and subsequent tissue manipulation (Figure 28).

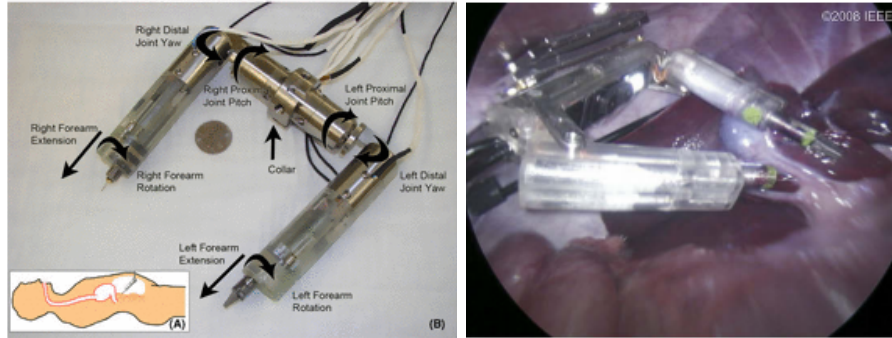


**Figure 28:** The Dexterous in vivo robot system developed by Lehman

- The **Miniature in vivo robotic platform for LESS** (LaparoEndoscopic Single-site Surgery) has been developed by Wortman, Dolghi et al. from University of Nebraska (26,28,29). Each arm consists of a two-degree of freedom rotational elbow joint. Specialized end effectors on each forearm can be interchanged to provide tissue manipulation, monopolar cautery, and intracorporeal suturing capabilities. Each outer module is connected to a center module that contains two cameras. Control of the robot arms is accomplished using two PHANTOM Omni (Figure 29).

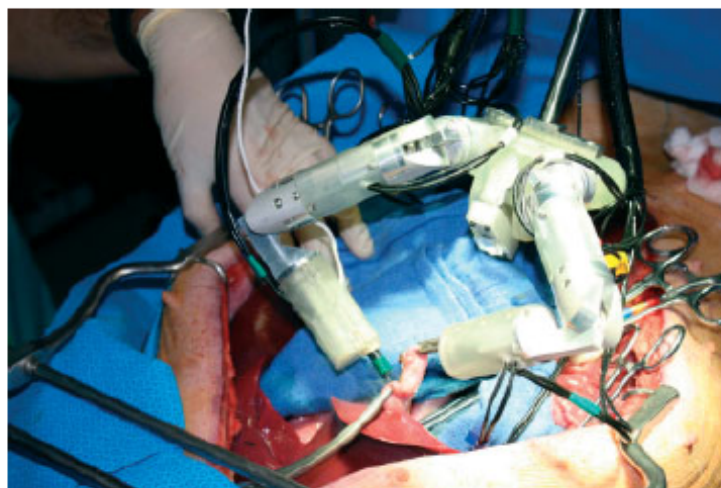


**Figure 29:** Miniature in vivo robotic platform for LESS setup in operative room

The two arms are 190mm in length and have a diameter of 26mm. Each arm has three degrees of freedom and rotational shoulder and elbow joints. The motors are embedded within the arms and body of the robot (Figure 30).

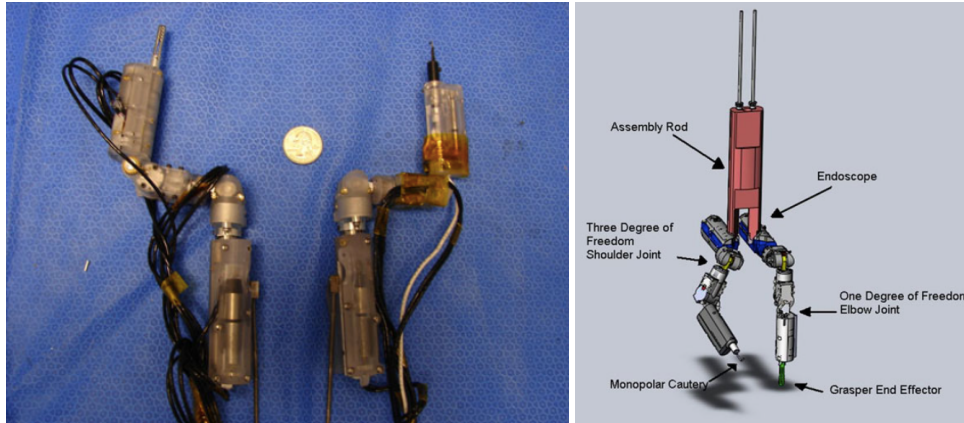


**Figure 30:** Miniature in vivo robotic platform for LESS robotic arms

- Each arm of the robot has six DOF (Figure 31). Each robotic joint is actuated using cordless permanent magnet, direct-current motors with magnetic encoders and controlled using a proportional-integral-derivative (PID) control method. This control is implemented by LabVIEW software (National Instruments Corporation, Austin, TX) and two CompactRIO motor drivers (National Instruments, Austin, TX, USA). The grasper (end effector) has an opening and closing force of 15 to 16 Newtons.

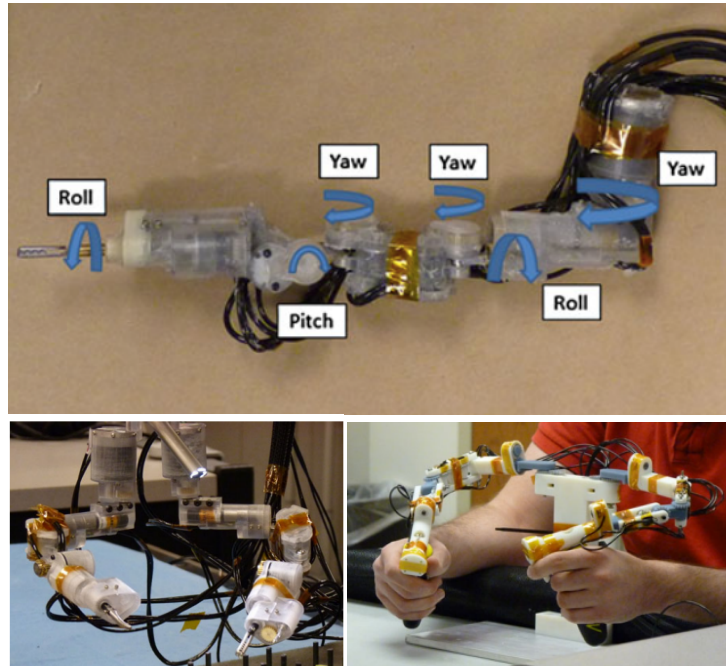


**Figure 31:** DoF of robotic arms and remote control

- The **single-port surgery robotic system** developed by Kobayashi, Liu et al. from Waseda University, Japan (32,33). The robot consists of a vision field control manipulator (robotic platform), two surgical tool manipulators and one flexible endoscope. The tool manipulators have six DOF for each arm. The diameter of the part that is inserted inside a patient's body is 25mm. The length of the arms is of 45mm and their diameters is 8mm. Two tool manipulators (in this case, a gripper and a cautery end-effector) are fixed in the forefront of the sheath manipulator (Figure 32).

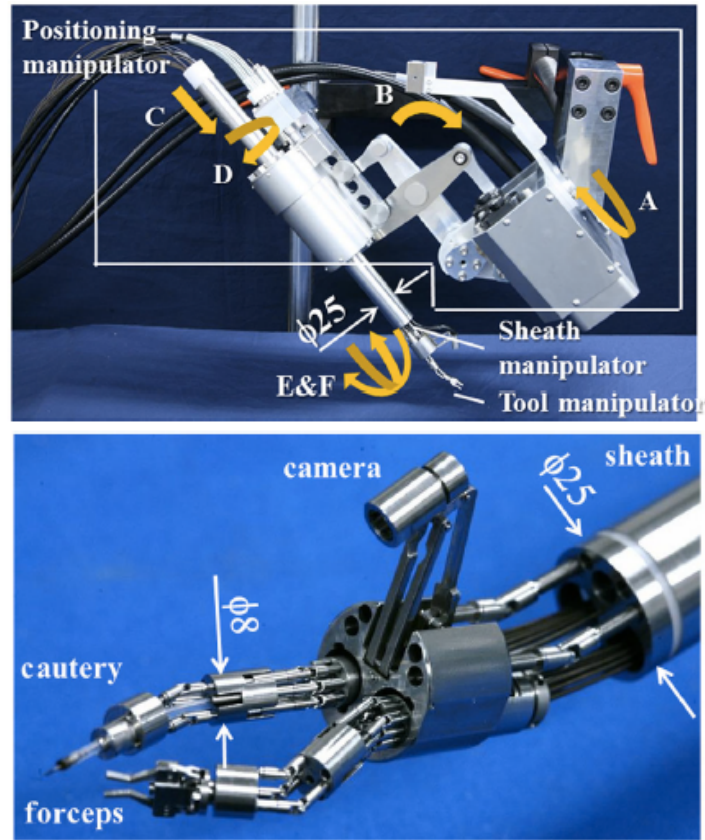


**Figure 32:** Single-port surgery robotic system developed by Kobayashi et al.

- Finally, Figures 33, 34 and 35 show an overview of Robots for Minimally Invasive Surgery already available on the market.



**Figure 33:** Virtual Incision





**Figure 34:** da Vinci Surgical System (Intuitive Surgical)

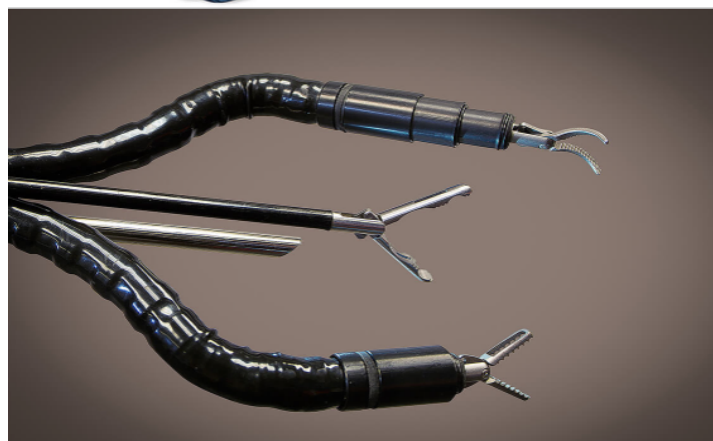


**Figure 35:** The SurgiBot System (TransEnterix)



**Figure 36:** SPORT Surgical System (Titan Medical Inc.)

## **Chapter 2**

# **RED: a new endoscopic robotic platform**

### **2.1 Aim of the research**

The treatment of colorectal cancer (CRC) represents one of the greatest challenges for national health systems worldwide, since they are one of the most frequent cause of death and they lead to substantial economic burdens. Today, thanks to screening programs, these neoplasms can be diagnosed early. This makes it possible for there to be a less invasive medical treatment with respect to major surgery, which can be obtained through local excision with an endoluminal approach.

The surgical techniques for treatment of early GI cancer are three. Endoscopic Mucosal Resection (EMR, for very early stage, limited only to mucosal layer) and Endoscopic Submucosal Dissection (ESD) are a flexible endoscopic method for the entire gastrointestinal (GI) tract, while Transanal Endoscopic Microsurgery (TEM) is a surgical technique for only the rectum tract, because its dimension and rigidity don't allow to get over the rectum-sigmoidal junction. However, while TEM technique is a really surgical procedure that respect the principles of counter-traction of tissues allowing a precision dissection, the endoscopic instruments available today do not generally allow surgical maneuvering

(manipulation, dissections, suture, etc.), with major risk of incomplete resection, bleeding and bowel perforation.

For these reasons the aim of the work is to develop a miniature robotic device that is designed to be coupled to a traditional flexible endoscope for the surgical dissection of gastrointestinal tract early neoplasms. The device includes a cap body with two robotic arms for performing manipulation and surgical tissue dissection. Each arm has three degrees of freedom, which is enough for this kind of application. The advantages in using this robotic device are various: a high operational accuracy and a complete lesion removal are guaranteed, an endoscopic room is enough, the patient does not undergo surgery under general anesthesia, and the hospitalization times and so the general hospital costs are significantly reduced.

## 2.1 Research overview

As a first step, we have analyzed surgical instruments with robotic arms, both endoscopic platforms available on the market that are still in the search stage. These technologies use dedicated tools with high purchase and usage costs. For this reason, we have decided to proceed with the development of an ex-novo robotic platform that can use a standard operating flexible standard endoscope with a maximum external diameter of 11.5mm. Typically, a robotic platform includes a set of units such as: robot device, outer box that contains part of the robot control, control PC, man-machine interface (*i.e.*, Phantom Omni).

This new robotic platform, developed in cooperation with The BioRobotics Institute of the **Scuola Superiore Sant'Anna** in Pisa, was called **RED** (Robot for Endoscopic Dissection).

At the tip of a standard endoscope a hood (RED) is placed with onboard miniaturized commercial motors that move two teleoperated robotic arms, diathermic hook and gripper (Figure 37). The endoscopist (surgeon A) holds the endoscope near the lesion, while the operator (surgeon B) drives the robotic arms through a remote control (Figure 38). The RED system is supported by an external platform, a personal computer and two Geomagic Touch Phantoms (3D System, Inc.).



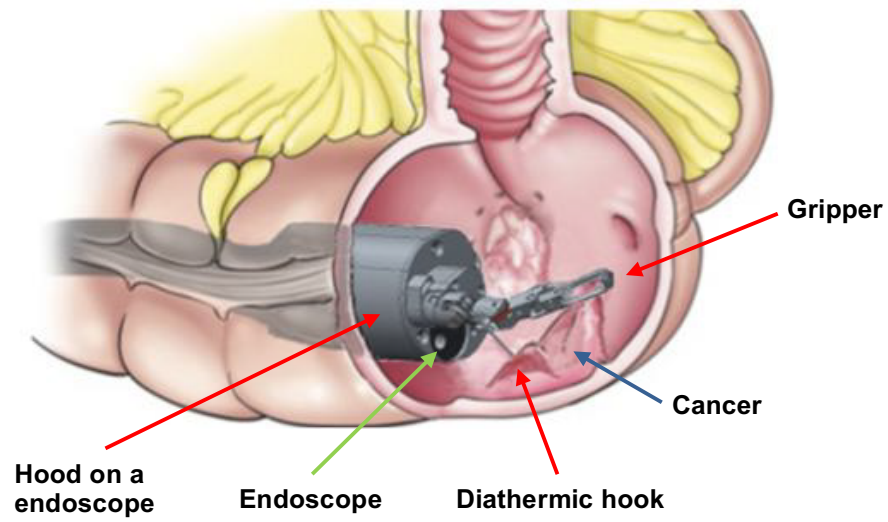


**Figure 37:** RED in operative position.

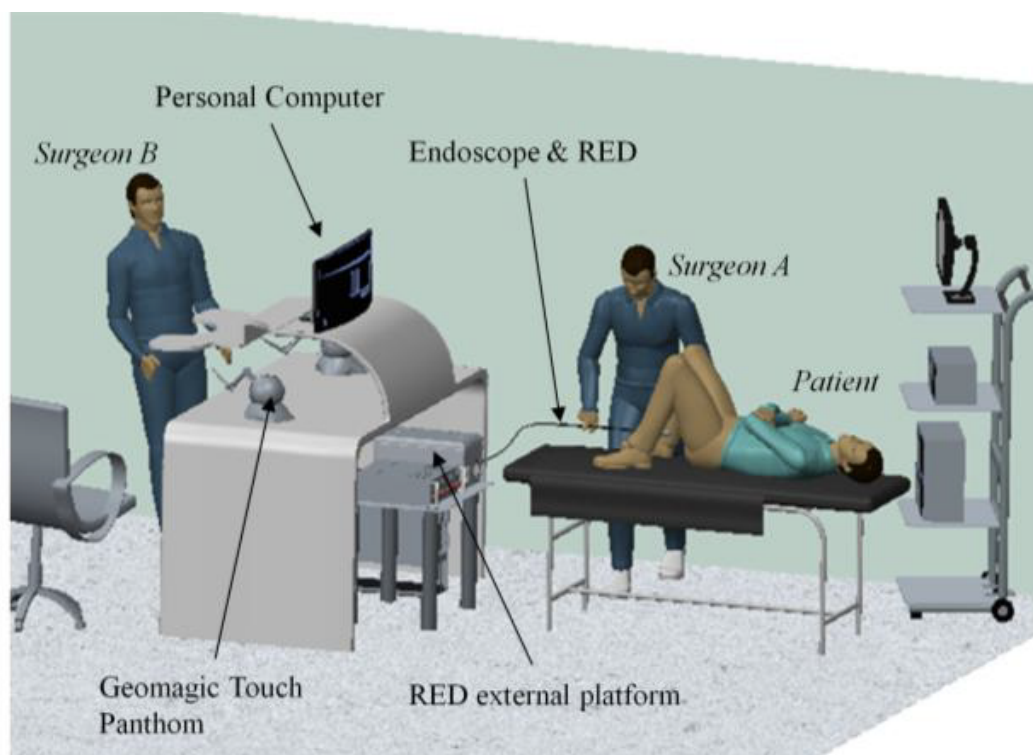


**Figure 38:** Rendering of the operative room.

# Chapter 3

## Materials and Methods

### 3.1 Identification of force value

The evaluation of the involved forces during typical surgical procedures is crucial for setting the design specifications (*i.e.*, choice of actuators, reduction stages, need for gearboxes or pulleys, and thus the overall dimensions) of new medical robotic devices, self-standing, or for integration on a standard endoscope.

During the tissues manipulation to perform dissection, two types of forces are applied: a lifting force and a traction force (Figure 39).

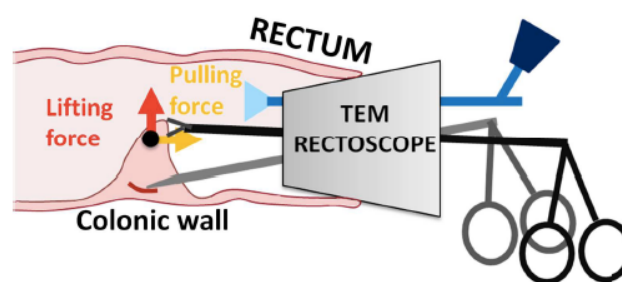


**Figure 39:** Lifting and pulling force during dissection

By using TEM instrumentation, a preliminary test was performed to identify the minimum force threshold value that the gripper must develop to perform the dissection. Forces exerted by surgeons for lifting and pulling rectal tissues were measured both ex-vivo and in-vivo. In order to replicate the same conditions

experienced by surgeons, an endoscopic grasper routinely used for TEM was adapted using a force measurement tool developed by Ranzani et al (36).

A scheme of the force measurement system is shown in Figure 40. The system is composed of two parts: one fixed close to the surgical tool's handle and another close to the rectoscope.

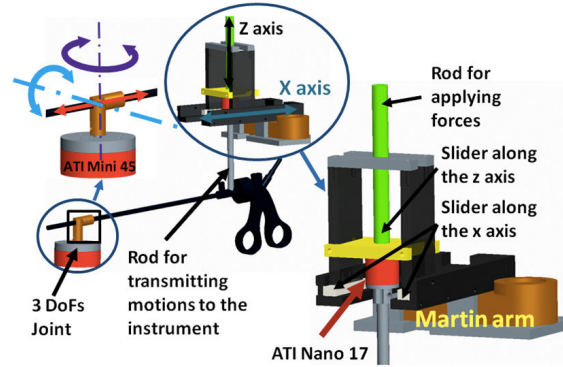


**Figure 40:** Scheme of force measurement system

The part close to the handle of the instrument has the function of constraining the trajectory of the surgical tool along the x (pulling) or z (lifting) axis and measuring the force directly applied by the surgeon to the instrument. The whole system is held by a 6-degree-of-freedom (DoF) passively orientable arm (Martin Arm, Martin GmbH & Co., Tuttlingen, Germany) that can be fixed to the operating table. The design of this part of the system is shown on the right side of figure 2. A 6-axis F / T sensor (NANO17, ATI, USA, resolution = 0.00625N) is connected to the slider (yellow in the picture) that constrains the motion along the z direction by means of guiding grooves. Forces are applied by the surgeon using a rigid rod (green in the picture). The position of the slider along the axis can be fixed at different heights by means of four screws. Translation along the x axis can be obtained by shifting the whole slider for the z axis along the x direction. All components are fabricated in Delrin® and Aluminum; the sliding parts for the x axis slider are produced in Teflon to reduce friction and their motion is constrained by aligning the grooves as for the z axis slider.

The motions imposed with the sliders are transmitted to the surgical tool by means of a rigid rod (shown in grey in Figure 40). The rod is simply tied to the surgical instrument with an inextensible wire. This coupling strategy allow an

easy connection between the surgical tool and the measuring system without constraining the relative reorientation between the tool and the rod.

The part close to the surgical TEM rectoscope (Figure 40, on the left) has the function of measuring the reaction forces on the instrument due to the fulcrum effect of the access trocar. It is composed by a tripod (not illustrated in Figure 40) used for positioning the system at the correct height with respect to the TEM rectoscope, a 6 axis F/T sensor (MINI 45, ATI, USA, resolution = 0.025N) and a 3 DoF joint for guiding the instrument shaft. Such joint allows translation, for inserting the instrument, and two rotations (yaw and pitch) thus replicating the effect of the TEM rectoscope itself.

Both in the ex-vivo and the in-vivo tests, each surgeon was asked to perform an exposure of the endoluminal tissue using a 5 mm Johan endoscopic instrument (Microfrance, St Aubin, France). The procedure consisted of four different phases, in which the surgeon performed the surgical procedure acting on the system of Figure 41-a, as follows.

- 1) The surgeon inserted the sensorized laparoscopic tool through the rectoscope port, and positioned the tip of the instrument at about 80 - 120 mm from the rectoscope front plate with the instrument handle.
- 2) The surgeon approached the colorectal tissue with the grasper by applying the  $F_s$  on the rod along  $z+$  direction ( $F_t$  along  $z-$ ). The tissue was then grasped from the handle and the grasper locked.
- 3) The surgeon applied a force on the rod along  $z$  direction ( $F_t$  along  $z+$ ) in order to lift the endoluminal tissue until a good exposure of the tissue was obtained.
- 4) The surgeon, still using the same rod mentioned above, pulled the endoluminal tissue along  $x+$  direction ( $F_t$  along  $x+$ ).

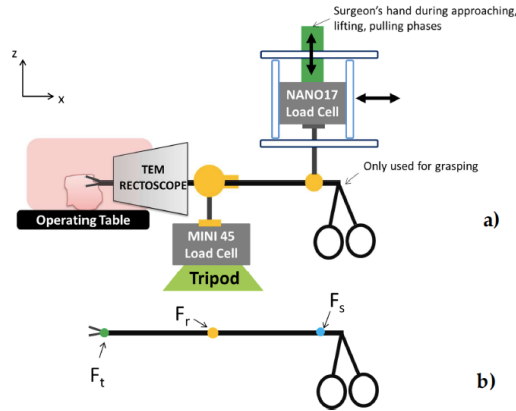


**Figure 41:** a) Scheme for the measurement setup. b) Corresponding involved forces;  $F_r$ ,  $F_s$ ,  $F_t$  can be along  $\pm z$  or  $\pm x$ .

Tests were conducted both ex vivo (suine bowel in TEO training box) and in-vivo (on ten domestics female pig).

### 3.2 Estimate of maximum external size of the device

Before proceeding with the development of the robotic device, it was necessary to establish its maximum dimensions that would allow progression through the colon. Therefore, a colon anatomy analysis is required to study the reference environment in which the device will be inserted. From the study of Alazmani et al. (37), the geometric characteristics of the various sections were extracted, in terms of length, diameter and angle of curvature (Figure 42, Tables 2 and 3).

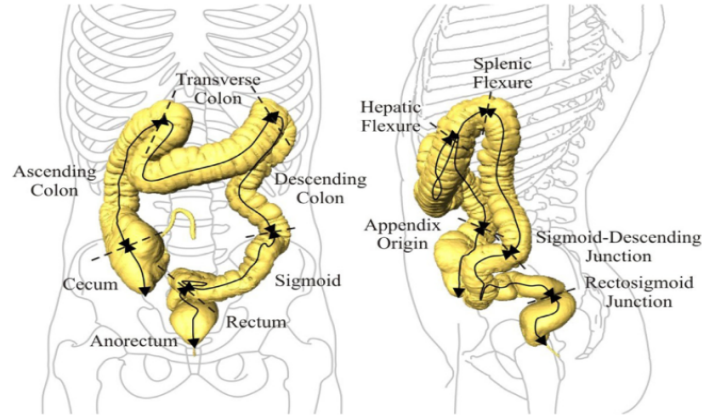


**Figure 42:** Schematic representation on colonic segment.

Comparison of the colonic segmental diameter in supine and prone orientations in 24 patients (mean  $\pm$  SD (median)).

	Diameter, cm		
	Supine	z-value (p)	Prone
Rectum	3.6 $\pm$ 0.8 (3.4)	-1.400 (0.166)	3.7 $\pm$ 0.7 (3.6)
Sigmoid	2.6 $\pm$ 0.4 (2.5)	-1.263 (0.214)	2.6 $\pm$ 0.3 (2.6)
Descending	3.3 $\pm$ 0.6 (3.3)	-1.072 (0.294)	3.2 $\pm$ 0.5 (3.1)
Transverse	3.7 $\pm$ 0.4 (3.7)	-2.030 (0.042*)	3.6 $\pm$ 0.5 (3.5)
Ascending	4.5 $\pm$ 0.7 (4.7)	-2.359 (0.017*)	4.3 $\pm$ 0.7 (4.6)
Cecum	4.4 $\pm$ 0.7 (4.5)	-3.187 (0.001*)	3.8 $\pm$ 0.6 (3.9)
Proximal colon	4.2 $\pm$ 0.4 (4.3)	-3.514 (0.000*)	3.9 $\pm$ 0.5 (4.0)
Distal colon	3.1 $\pm$ 0.5 (3.0)	-4.286 (0.000*)	3.1 $\pm$ 0.4 (3.1)
Total colon	4.7 $\pm$ 0.5 (4.7)	-4.286 (0.000*)	3.5 $\pm$ 0.4 (3.5)

**Table 2:** Comparison of the colonic segmental diameter.

Comparison of the colonic segmental angle (mean  $\pm$  SD (median)), skewness (s), and kurtosis (k) in supine and prone orientations.

	Supine		Prone	
	Angle, deg	Skew (k)	Angle, deg	Skew
Rectum	42.2 $\pm$ 27.3 (42.2)	0.03 (-0.84)	45.2 $\pm$ 28.1 (47.1)	-0.17 (-0.98)
Sigmoid	46.9 $\pm$ 24.2 (43.8)	0.44 (-0.58)	47.9 $\pm$ 24.1 (45.1)	0.34 (-0.71)
Descending	33.6 $\pm$ 21.1 (29.1)	0.84 (0.07)	36.1 $\pm$ 21.7 (31.0)	0.79 (-0.12)
Transverse	38.7 $\pm$ 23.3 (35.6)	0.42 (-0.80)	37.2 $\pm$ 22.9 (33.0)	0.51 (-0.69)
Ascending	30.2 $\pm$ 17.7 (27.1)	0.69 (-0.09)	31.8 $\pm$ 18.0 (29.7)	0.56 (-0.34)
Cecum	27.1 $\pm$ 15.5 (22.4)	0.54 (-0.49)	32.4 $\pm$ 15.9 (31.9)	0.42 (0.02)
Splenic*	31.5 $\pm$ 18.5 (27.4)	0.84 (0.25)	35.1 $\pm$ 20.4 (30.3)	0.74 (-0.17)
Hepatic*	51.8 $\pm$ 22.4 (52.5)	0.00 (-0.82)	51.6 $\pm$ 21.8 (50.8)	0.06 (-0.75)

**Table 3:** Comparison of the colonic segmental angle.

As shown in Tables 2 and 3, splenic flexure represents the most critical point for crossing of the endoscope: for this reason, a study was carried out with the support of CAD software to evaluate available space.

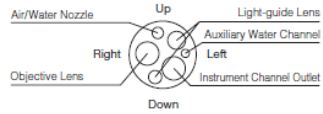

### 3.3 Assessment of the overall dimension: in-vitro tests and mock-up creations

The RED will be anchored at the head of a commercial endoscope. The initial idea is to have a device compatible with most endoscopes located in hospitals.

Surgeons usually have endoscopes that range from 9.2 to 9.9mm. The most common tools are:

- 9.9mm gastroscope (Olympus GIF-HQ190)
- 9.2mm gastroscope (Olympus GIF-H185)
- 9.7mm pediatric colonoscope (Olympus PCF-PH190L / I)

Figure 43 shows an example of endoscope data sheet with its main features.

Optical System	Field of view	Normal 140°
		Near 140°
	Direction of view	Forward viewing
	Depth of field	Normal 5-100 mm Near 2-6 mm
Insertion Section	Distal end outer diameter	9.9 mm
	Distal end enlarged	
		
	Insertion tube outer diameter	9.9 mm
	Working length	1030 mm
Instrument Channel	Channel inner diameter	2.8 mm
	Minimum visible distance	3.0 mm from the distal end
Bending Section	Direction from which endotherapy accessories enter and exit the endoscopic image	
	Angulation range	Up 210° Down 90° Right 100° Left 100°
	Total Length	1350 mm
	Compatible EVIS EXERA System	Video System Center OLYMPUS CV-190 Xenon Light Source OLYMPUS CLV-190

Dual Focus images courtesy of Roy Soetikno, MD.  
NBI images courtesy of Horst Neuhaus, MD.

**Figure 43:** Example of Data Card for Olympus GIF-HQ190 Gastroscope

As a reference, the pediatric colonoscope "Olympus PCF-PH190L / I" has an outer diameter of 9.7mm (this is the diameter stated by the datasheet but in practice the diameter to be considered is 11.5mm).

Therefore, at the design level, a maximum external diameter of the endoscope of 11.5mm was considered and the possibility of adapting the hood to endoscopes with different diameters.

Using the PTC Creo 2.0 Software, the pediatric colonoscopy was reproduced, including the visual field (Figure 44).



**Figure 44:** The darkest point at the tip represents the rigid and non-flexible endoscope cap. The yellow cone is instead the field of vision.

The RED will consist of a hood positioned at the tip of a commercial endoscope and consist of two robotic arms (diathermic hook and gripper) to perform a colon submucosal dissection procedure (from rectum to cecum). Starting from the CAD reproduction of the endoscope size, knowing the maximum size of RED that will be placed on the tip, now it is possible to design the not working preliminary prototype (mock-up) to perform the first in vitro tests in order to evaluate the overall dimensions.

The aim of the **in-vitro tests** was to define the following 2 aspects.

1) The maximum size that a cylindrical cap (representing the RED) anchored to an endoscope may have. The cap should not limit the movements of the endoscope tip and at the same time should not be cumbersome in order to maintain the ability to cross all the various colon angles (in particular the splenic flexure that representing the most critical curve) and reach the cecum.

As a first step, a cylindrical cap (representing RED) in Delrin<sup>®</sup> has been made with various lengths and diameters (Figure 45).



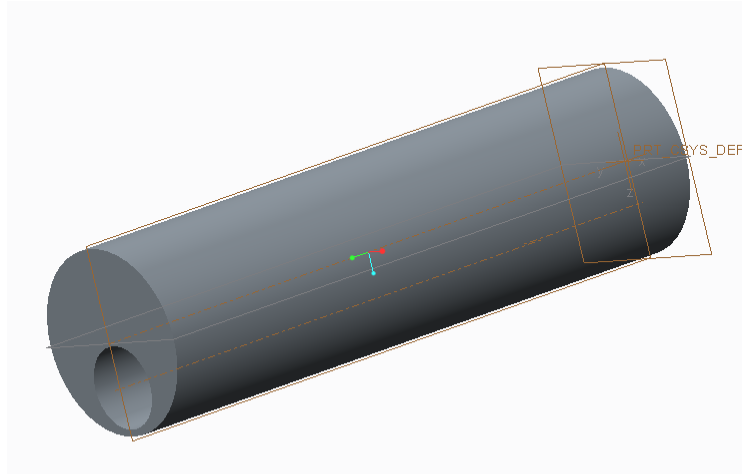


**Figure 45:** Cylindrical cap representing RED

Five different cylinders were made in the following sizes:

- length = 100mm and outer diameter = 28mm;
- length = 80mm and outer diameter = 28mm;
- length = 60mm and outer diameter = 28mm;
- length = 100mm and outer diameter = 26mm;
- length = 60mm and outer diameter = 30mm.

Inside there is a housing for the endoscope (central channel diameter of 11.5mm and widening to 12.5mm in the end to not limit the movements of the endoscope). For all selected combinations, we decided to hold the diameter fixed and only change a parameter (in this case the length). In addition, we have added two limit cases: maximum length with minimum diameter and vice versa. The length of 100mm was chosen because in the case of choosing a system with 4 degrees of freedom, this represents approximately the length required. While 60mm represents the indicative length for two robotic arms with 2 degrees of freedom each. As for the outer diameter, as shown by the previous tests, there is no margin of change: therefore, it was fixed at 28mm. As a reference endoscope, the pediatric colon is used, considering, as mentioned above, an outside diameter of 11.5mm.

2) The degrees of freedom (DoF) of the two robotic arms sufficient to make a submucosal dissection across the colon. The possibilities analyzed were:

- a) 4 DoF arms;
- b) 2 DoF arms (roll and pitch at the base);
- c) 2 DoF arms (pitch at base and tip roll);
- d) 1 DoF arms.

Each header solution was designed with CAD and later the corresponding mock-up with 3D printer was created to perform the in vitro test. Below are the four solutions tested for the robotic arms and the option chosen based on the test results. The prototypes diameter is 14.5mm with a length of 90mm.

*a) Arms with four degrees of freedom*

In this version, first was designed and then built a mockup consisting of a base (placed at tip of the endoscope) and two segments of the robotic arm with the following degrees of freedom (in succession): roll-pitch-pitch-roll (Figure 46).

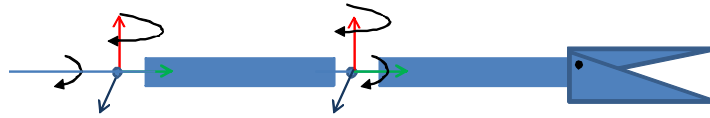


**Figure 46:** Scheme of 4 DoF robotic arms

Different prototype grippers have been printed with different angular field of the joints:

- *Base solution:* roll angle (0 - 90°), pitch ((-60°) - (60°)), pitch (0-90°), roll (0 - 90°);
- *Increased solution by 20°:* each degree of freedom has 20° rotation greater than the base for each joint;
- *Reduced solution by 20°:* each degree of freedom has 20° rotation less than the base for each joint.

There was only one mockup for the diathermic hook with the same degrees of freedom and angular range of the basic gripper solution.

In addition, a base for both arms (gripper and diathermic hook) has been built with a decentralized hole for the endoscope passage. Below are shown CAD assembling (Figure 47) and the mock-up (Figure 48) of the various components using robotic arms with 4 DoF.

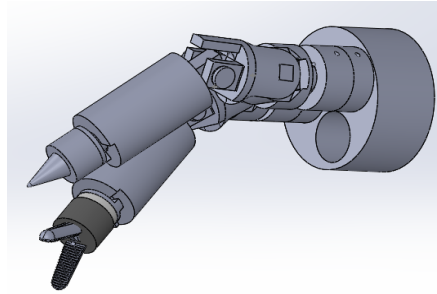


**Figure 47:** CAD assembling with 4 DoF

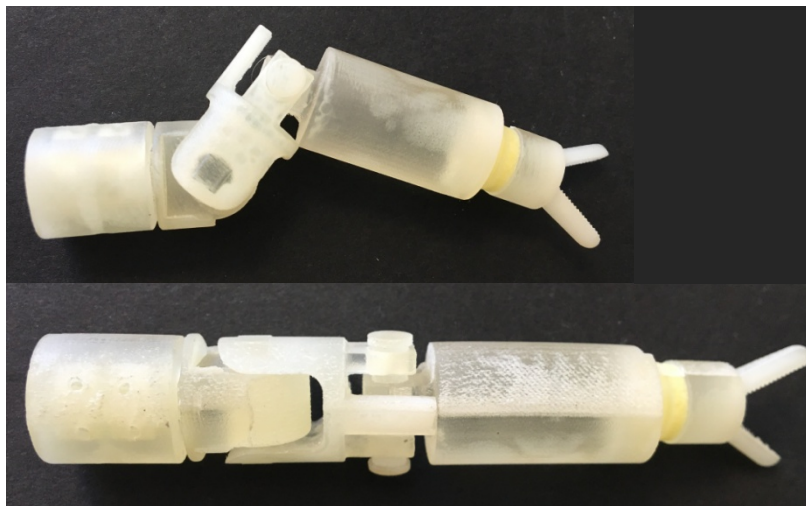


**Figure 48:** Mock-up assembling of robotic arm with 4 DoF

*b) Arms with two degrees of freedom: roll and pitch*

There has also been a solution with only two degrees of freedom. The DoF order in this mock-up is roll and pitch, both placed at the base of the arm (Figure 49).



**Figure 49:** Scheme of 2 DoF placed at the base of robotic arm

Two arms were made, representing the gripper and cauterizer with a roll at the base of  $360^\circ$  and a pitch of  $180^\circ$ . The arms have precurved distal portion to try to compensate for the lack of other degrees of freedom. Figure 50 shown the CAD assembly, composed of gripper arm, diathermic hook arm and base.

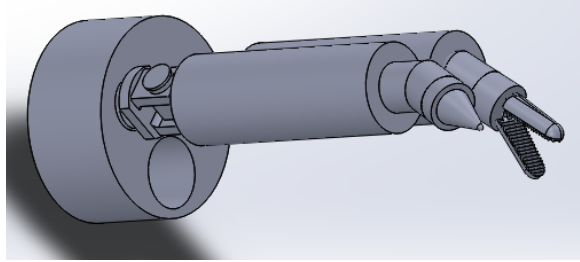


**Figure 50:** CAD assembly

*c) Arms with two degrees of freedom: pitch and roll*

The same previous mockups were made, but the order of degrees of freedom was reversed: the pitch at the base and the roll in the tip. (Figure 51).

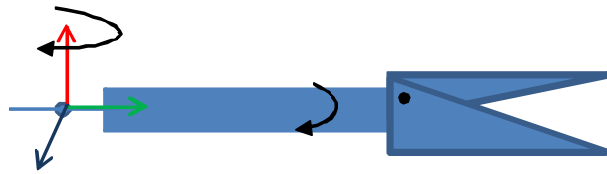


**Figure 51:** Scheme of 2 DoF with roll at the tip of robotic arm

Considering that the system does not have the roll at the base, it is best to choose immediately a position to align the arm during the pitch in the correct direction (Figure 52).

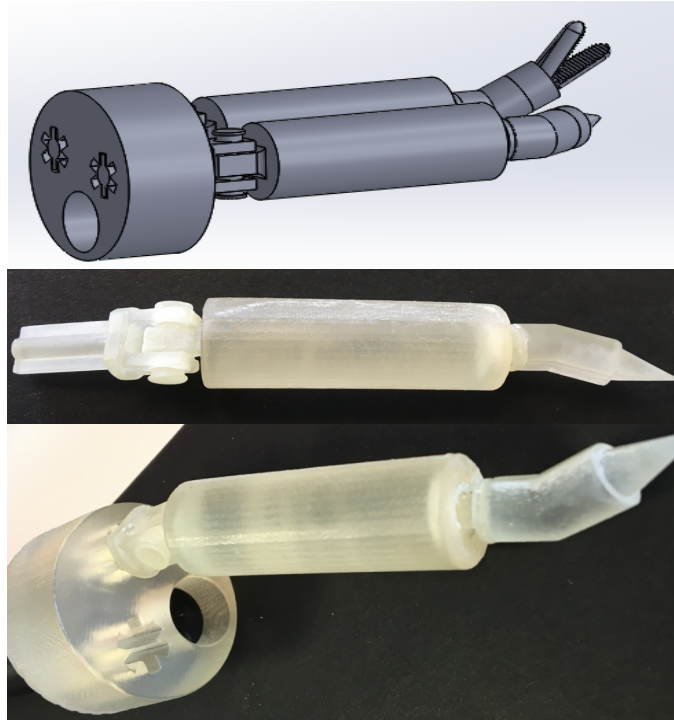


**Figure 52:** CAD and Mock-up assembly of 2 DoF robotic arm with roll at the tip

*d) Arms with one degree of freedom*

One mockup has also been made with one degree of freedom: pitch at the base of robotic arm (Figure 53).



**Figure 53:** 1 DoF robotic arm

In this case, two robotic arms (gripper and diathermic hook) have been made with interchangeable tips. The tips vary by degree of curvature (i.e.  $30^\circ$  and  $60^\circ$ ) and the length of the support that hold up the tool (Figure 54).

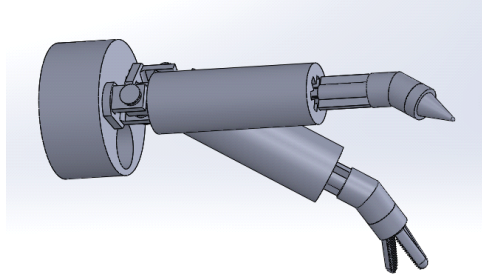


**Figure 54:** CAD design of 1 DoF robotic arm

The tip can change the position in different angles so you can understand which one is the best configuration using a single mockup (Figure 55).

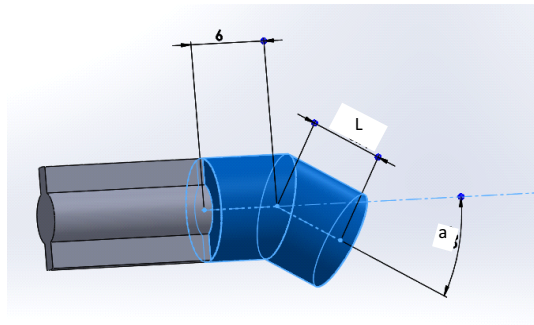


**Figure 55:** angles position of diathermic hook

Various tips made:

- $\alpha = 30^\circ$ ;  $L = 5.77\text{mm}$
- $\alpha = 30^\circ$ ;  $L = 10\text{mm}$
- $\alpha = 60^\circ$ ;  $L = 10\text{mm}$
- $\alpha = 60^\circ$ ;  $L = 14\text{mm}$

The length of the diathermic hook is 13mm and the gripper length is 17mm

# Chapter 4

## Results

### 4.1 Identification of force value

The results of preliminary test of force measurement for lifting and pulling the tissue are showed in Table 4 (36). Based on these results we have established that the minimum force that the gripper will have to develop by push-pull is 1.5N.

	Trials	Lifting force (N)	Range of lifting forces (N)	Pulling force (N)	Range of pulling forces (N)
<i>Ex-vivo</i>	50	$1.14 \pm 0.26$	0.66 – 1.53	$0.93 \pm 0.30$	0.36 – 1.43
<i>In-vivo</i>	10	$0.89 \pm 0.21$	0.59 – 1.21	$0.58 \pm 0.31$	0.18 – 1.09

**Table 4:** Summary of the forces measured in the in-vivo and ex-vivo tests.

### 4.2 Estimate of maximum external size of the device

The result of study with the support of CAD software to evaluate available space at level of splenic flexure (corresponding at the smallest angle of colon) is showed in Figure 56.

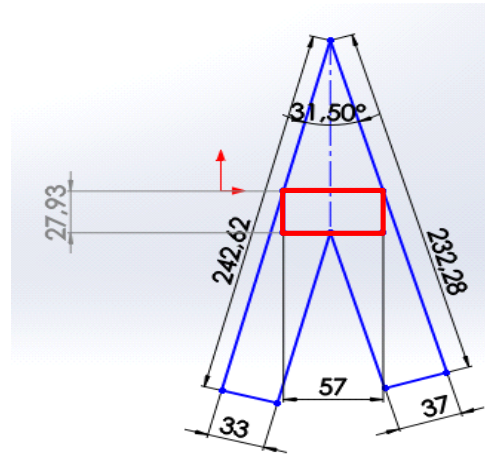


**Figure 56:** CAD design of splenic flexure. The red rectangle represents the maximum size that allows to cross the flexure.

In the drawing were fixed:

- diameter of descending length: 33mm;
- transversal diameter: 37mm;
- splenic flexion angle:  $31.5^\circ$ ;
- cap length + residual colonoscope flush during the curve: 57mm.

With this data, you get a maximum possible diameter of the cap of 28mm.

Thanks to this preliminary study it was possible to establish the relationship between the two maximum dimensions of the RED (diameter and length): depending on the required characteristics, changing the length of the rigid part it is possible to obtain the maximum diameter of the RED while maintaining the possibility of reaching up the cecum.



### 4.3 Assessment of the overall dimension: in-vitro tests and mock-up creations

Three in vitro feasibility tests were conducted, each for the three main components: hood, gripper arm, hook arm.

#### 4.3.1 Flexibility test with hood

The total final size of the hood will be approximately 26mm in diameter and 50mm in length. During the flexibility test it has been seen that a cap of this size, if pointed at the colonoscope, does not limit the movements (Figure 57). The outer diameter of the cap will undergo a cut (to the maximum of possibilities) to lighten and diminish the entire structure.



**Figure 57:** Flexibility test with cap 26mm diameter and 50mm length.

Within the hood there will be two separate bases, containing the two robotic arms and the space for the colonoscope. The base sliding will be carried out with cable implementation. By separating the two bases of the arms, allowing an independent sliding, the degrees of total freedom of the system increase. This choice greatly facilitates the use of the cauterizer: this, having both degrees of freedom at the tip of the arm during the "operative position", may also remain partly within the cap, and therefore vary the distance on which to act.

### 4.3.2 Workspace definition tests

The tests were conducted in order to find the right compromise between the sophistication in the articulation of the robotic arms (to allow the right tissues manipulation) and the need to contain mechanical complexity to minimize the size of the compartments.

For each experimented solution, first the CAD prototype was designed, then the corresponding mock-up was created and finally tested.

#### 4.3.2.1 DoF of gripper robotic arm

The tests have shown that the most effective solution for this robotic arm is that it has two degrees of freedom: pitch at the base and tip roll (Figure 58). The motors used for the movements of this arm are all external.

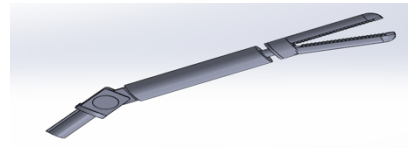
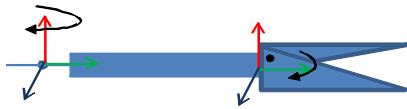


**Figure 58.** Representing degrees of freedom, CAD design and mock-up of gripper robotic arm

This combination of motors has been chosen because the gripper must exert more force than the cauterizer (the cauterizer can cut the tissue only if it is in traction). With the pitch at the base of the arm you can get a larger workspace, while with the tip roll, you have a lower strength loss as the force arm is less.

Regarding gripper, a classic laparoscopic fenestrated gripper has been taken as a model, with only one side opening; the clamping force will be executed by cables (Figure 59).



**Figure 59:** Classic laparoscopic fenestrated gripper

The gripper represented in the mockup does not have the central fenestrature, this choice was taken not to lighten the structure and therefore have the security that the 3D machine could print the mockup. In the final prototype the integrated gripper will be fenestrated and with unilateral opening as shown above.

#### 4.3.2.2 DoF of diathermic hook robotic arm

In this case, the tests have shown that the most effective solution for this robotic arm is that it has two degrees of freedom: both pitch and roll at the tip of the arm (Figure 60).

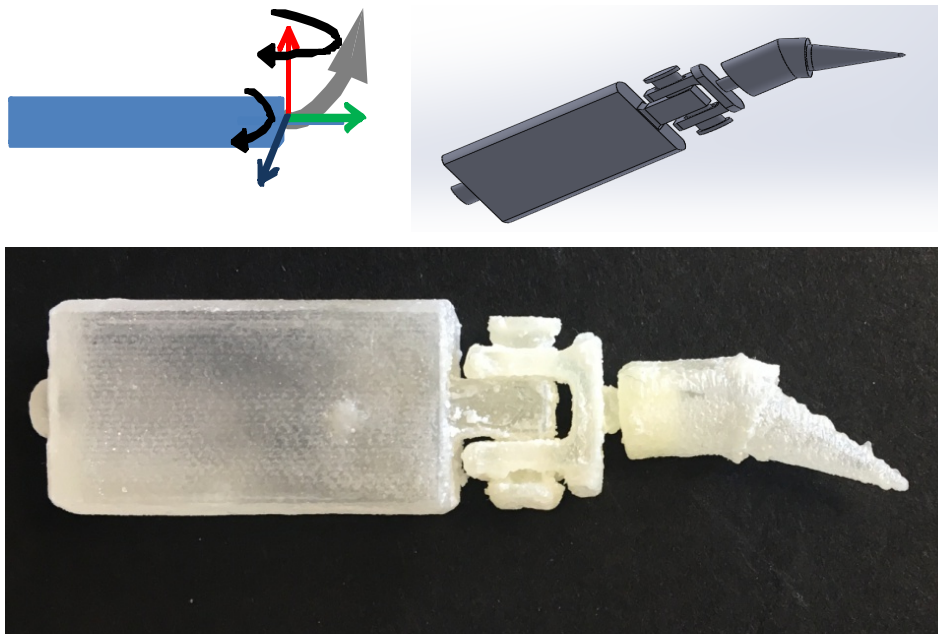


**Figure 60:** Representing degrees of freedom, CAD design and mock-up of diathermic hook robotic arm

In this arm, two engines with a diameter of 4mm each will be integrated, which is why they decided to put both degrees of freedom close to the tip: the forces generated by these motors are not high, thus minimizing the length of the arm of force application maximizes the tip force to the cauterizer.

The tip of the cauterizer will be curved up to the maximum of possibilities, always ensuring that the arm remains inside the cap shape. A traditional cauterizer used for TEM will be used.

The first mock-up assembly, based on these choices, is shown in Figure 61.

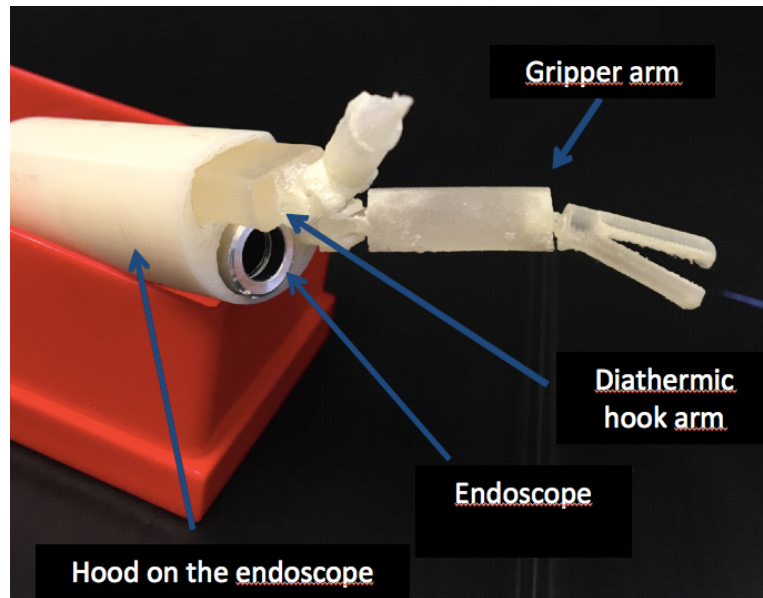


**Figure 61:** First mock-up assembly

Unfortunately, when the mock-up assembly was made, the gripper arm was not functional due to space problem in the engine installation that would allow the two DoF expected. Therefore, it was chosen to use a single DoF for gripper arm (with pitch at the base) associated with sliding inside the hood to eliminate the motor (Figure 62).



**Figure 62:** Scheme of gripper arm with pitch at the base and sliding (green arrows)

#### 4.3.2.3 RED final design and in-vitro test for workspace assessment

Previous tests have made it possible to identify the specifications for mechanical design. Below are the features of the four main RED elements, their assembly and the in vitro test to assess whether the field of work and vision are sufficiently wide.

##### 1) *Gripper arm*

The gripper arm is 42mm long and has a quadrangular section with a 6mm side and beveled corners with a bending radius of 2mm (Figure 63). It is characterized by two DoF: pitch at the base of the gripper and sliding inside the cap. The movements of the gripper robotic arm (pitch, sliding and gripper closure) are operated by three external motors through cables contained in a sheath adherent to colonoscope, while the opening of gripper is guaranteed by a spring (Figure 64). The gripper arm is expected to generate around 3N of lifting force and 10-14N of gripping force.

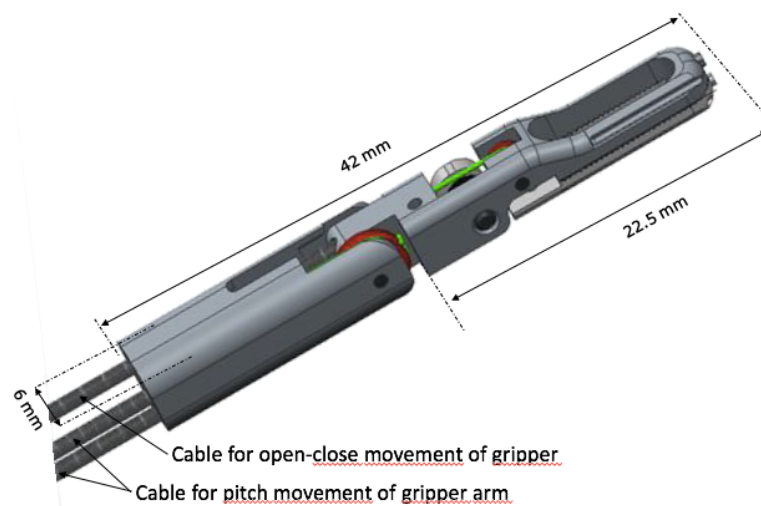


**Figure 63:** CAD design of gripper arm

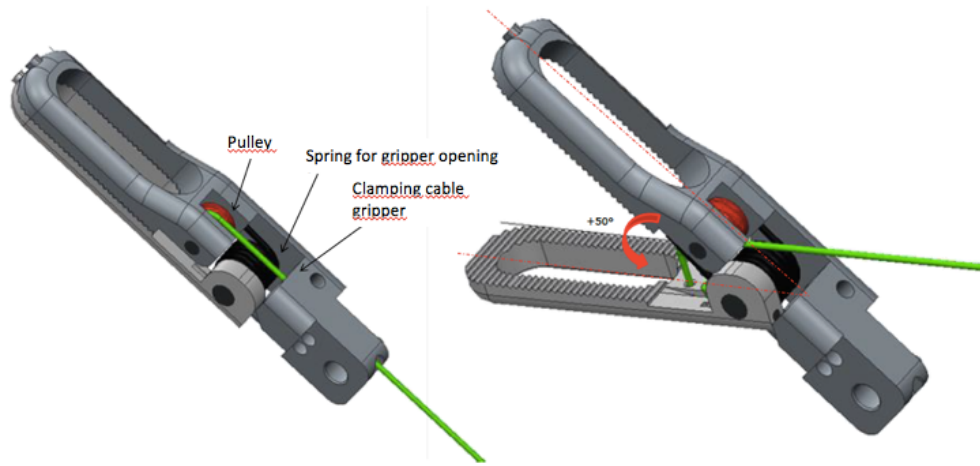


**Figure 64:** CAD design of gripper movement

One part of the gripper will be coated with a 0.5mm plastic cap (PEEK) to prevent that the tip of diathermic hook touching the metal directly and then conducting current. The transparent blue part of the Figure 65 represents the gripper hood.

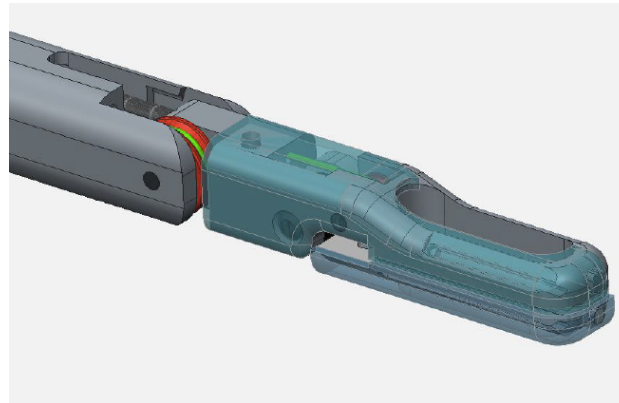


**Figure 65:** CAD design of the plastic gripper hood

## 2) Diathermic hook arm

The diathermic hook arm is 48.8mm length, 14.5mm wide and 7.5mm thick. The tip is equipped with a cauterizer of 13.7mm length and with a bend angle of  $110^\circ$  (Figure 66). The cauterizer will be made of titanium and will rest on a plastic

support to ensure electrical insulation between the tool and the rest of the robot. The length of the cauterizer has been fixed considering that the toe must touch the plane of the lesion and its working space must overlap (in part) with that of the gripper arm.

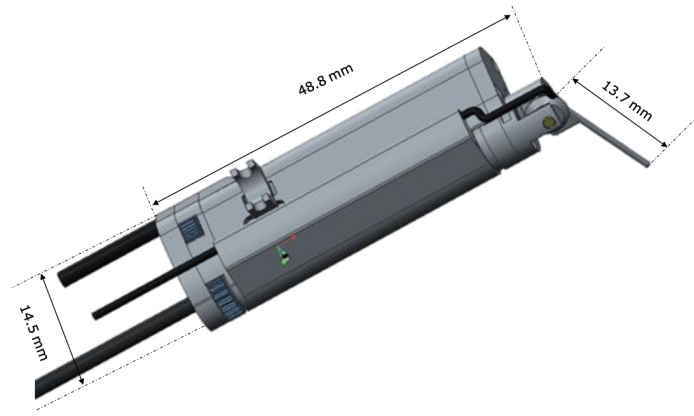


**Figure 66:** Diathermic hook arm

The arm is characterized by 3 DoF: pitch and roll at the tip and sliding of the entire arm. All degrees of freedom are obtained with integrated motors inside the RED: two directly on the arm and one (to slide) into the hood (Figure 67). The diathermic hook arm is expected to generate around 1,5N at the cautery tip.

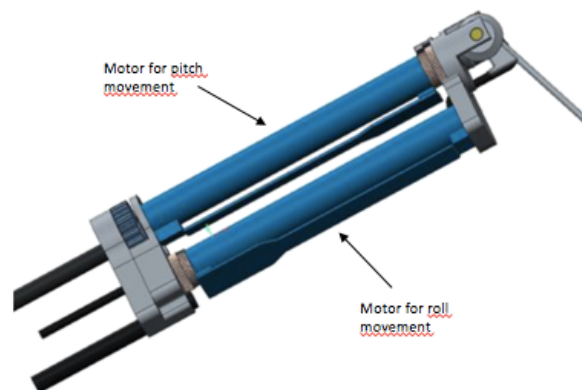


**Figure 67:** Internal view of diathermic hook arm with the position of the two motors

### 3) Hood

The hood serves to hold inside the two robotic arms and some mechanisms for the operation of the RED.

The actual length of the cap is 51mm and the outside diameter is 27mm but with a cut on the top that reduces its final diameter (Figure 68).

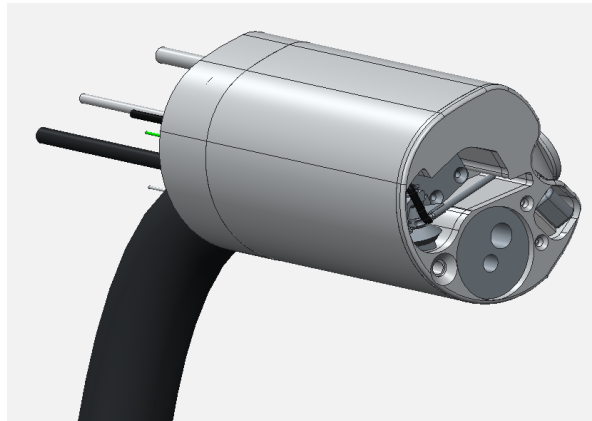


**Figure 68:** CAD design of the hood

### 4) External platform

The external platform includes all motors (with reducers and drivers), sensors, mechanical parts and electrical connections for RED movements. The platform will be placed inside a commercial box of external dimensions 280mm x 280mm x 130mm.

Based on the technical specifications described above, 3D mock-ups of the individual parts have been made, assembled and installed on an endoscope (Figure 69 and 70).



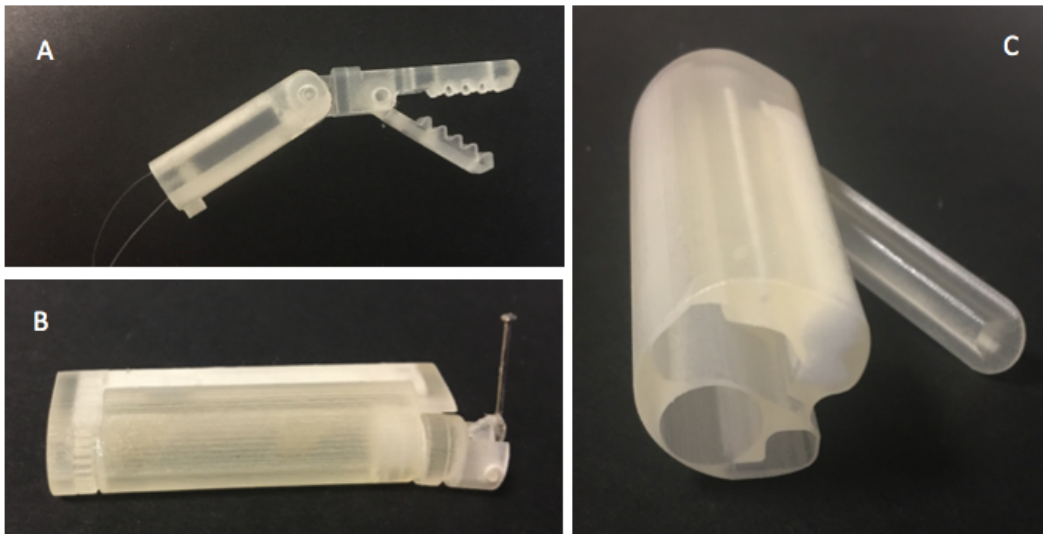


**Figure 69:** Definitive mock-ups. A) Gripper. B) Diathermic hook. C) Hood.

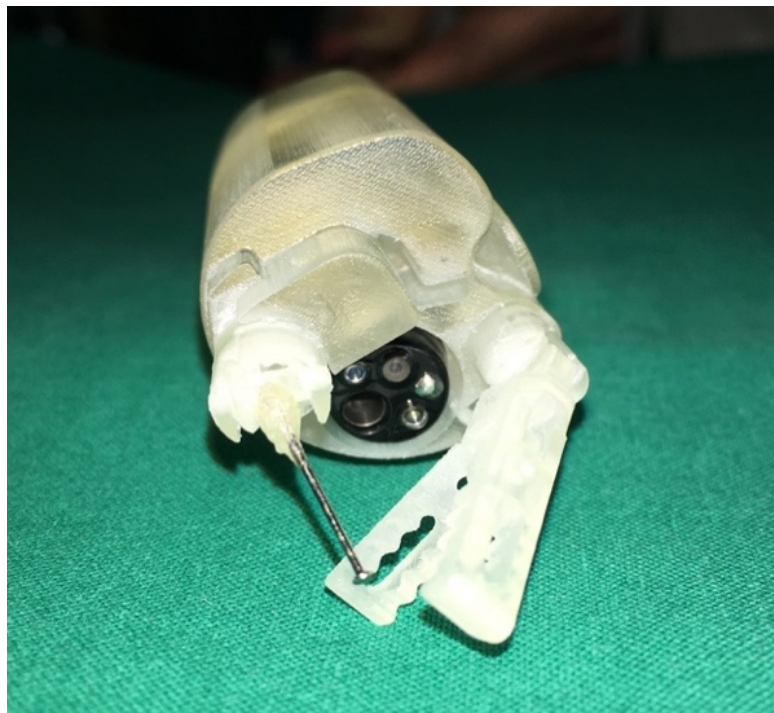


**Figure 70:** RED assembled and installed on an endoscope

With the model thus realized in scale 1:1 it was possible to perform the in vitro test to assess the workspace and vision using a pelvic trainer for TEM.

As shown in Figure 71, the operating field vision is not obstructed by the hood and the working range is sufficiently wide to perform a dissection.

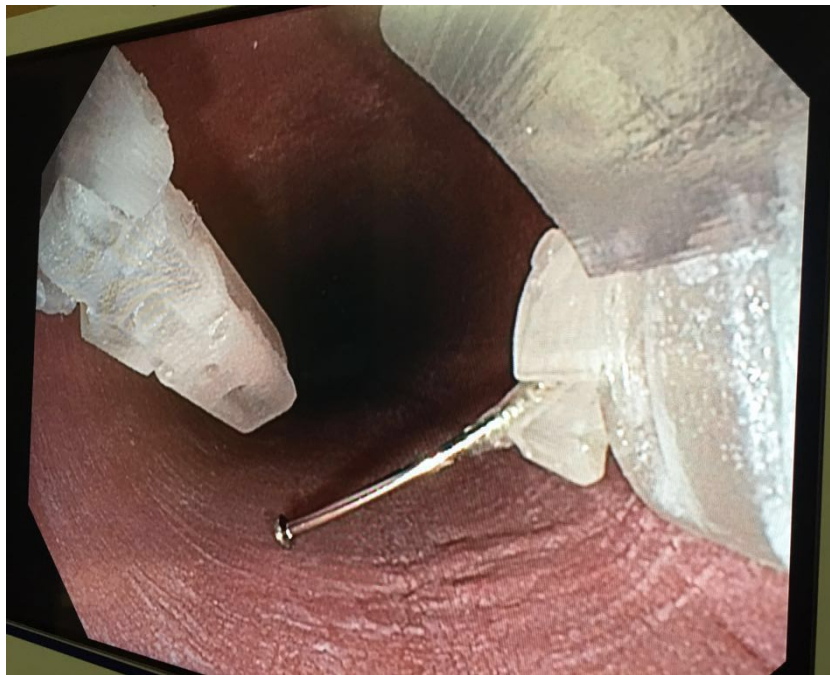


**Figure 71:** RED operative vision

# Chapter 5

## Discussion

Colorectal cancer (CRC) is the third most common cancer in males and second in females, and the fourth most common cause of cancer death worldwide. The implementation of screening programs and the use of colonoscopy has allowed to the identification of an increasing number of early-stage neoplastic lesions (1).

Presently, superficial colorectal neoplasms (including precancerous lesions and early cancer) can be resected in the colon by Endoscopic Mucosal Resection (EMR) and Endoscopic Submucosal Dissection (ESD), which in the rectum by Transanal Endoscopic Microsurgery (TEM), all minimally invasive technique, and have become the preferred choices (2).

TEM technique offers the advantages of superior visualization of the lesion and greater access to distal lesions with lower margin positivity and specimen fragmentation and lower long-term recurrence rates over traditional transanal excision (7), but it cannot be used in the proximal colon to the recto-sigmoid junction as the instrument is not flexible, so it cannot progress through the colon. In contrast, EMR and ESD techniques (5,6), which utilize a colonoscope, can be used to treat early lesions located throughout the colon but only for small size lesions and with a limited "en-bloc" excision rate, with risk of perforation of the bowel and higher local recurrence rate.

The challenge of carrying the TEM experience to perform dissections for early neoplastic lesions throughout the colon, overcoming its anatomical and technical limitations, has been collected by many authors, research institutes and

biomedical industries. The proposed solutions include dedicated endoscopic platforms (mainly developed by industries already active in the field of endoscopy), research devices and articulated robots (8-35). However, all these proposals, regardless of their effectiveness, have in common the development of platforms expressly designed for this use, with significant purchasing and management costs.

In order to contain management costs and especially purchasing costs, our research goal is to develop a robotic platform that could exploit a common operating colonoscope as a "scaffolding" that allow to treat lesions throughout the colon. The requirement to be respected, borrowed from the TEM experience, must be to be able to manipulate the tissue to allow the traction needed for a surgical dissection. This new robotic platform, developed in collaboration with BioRobotics Institute of the Scuola Superiore Sant'Anna (Pisa), was called RED (Robot for Endoscopic Dissection). At the tip of a standard endoscope a hood (RED) is placed with onboard miniaturized commercial motors that move two teleoperated robotic arms: the endoscopist holds the endoscope near the lesion, while the operator drives the robotic arms through a remote control.

The constituent elements of the developed robotic platform include a miniaturized robot device, an external box equipped with motors, driver and related mechanics, a control PC and two man-machine interfaces (i.e. Phantom Omni). The miniaturized robot has been designed to be coupled to the tip of traditional flexible endoscopes of about 11.5mm in diameter. The robot exploits the flexibility of the endoscope for navigation through the intestine and integrates 2-actived robotic arms (i.e. diathermic hook and gripper) extending the degrees of freedom (DoF), and thus enhancing the efficiency during complex task such as manipulation and surgical tissue dissection.

The "ex-novo" components design involved CAD design and subsequent 3D mock-ups with various technical solutions that are subsequently tested to get what we thought the solution with the best compromise between size and versatility of the robotics arm. At the end of this phase, the final prototype was assembled to perform an in-vitro test.

The first performed test analyzes the values of forces involved during dissection operations, since these values are crucial for setting project specifications. The purpose this study was to determine the required force value for lifting and pulling maneuvers using a TEM instrument to which a dedicated

force measuring device was applied (36). Thanks to this study, we have determined that the minimum force that the gripper will have to develop with the push-pull is 1.5 N: this is the value that will allow choosing the power of the motors that will move the robotic gripper arm.

Before proceeding with the design, it was necessary to establish the maximum dimensions of the RED hood that would allow its progression through the colon. From the study of Alazmani et al. (37) on the colon anatomy, we have extracted the geometric size of the various sections, in terms of length, diameter and angle of curvature. Splenic flexure is the most critical point for the progression of the endoscopic instrument. Starting from these data, we have reproduced to the CAD the maximum dimensions the hood must have to overcome this point, identified with a maximum diameter of 28mm and a maximum length of 57mm.

Once the relationship between length and outer diameter of the hood has been identified, a flexibility test was carried out to fix final dimensions that would not compromise the endoscope tip movements. The total final size of the hood will be approximately 26 mm in diameter and 50 mm in length.

Established the maximum size of the hood, we have tested the various possible solutions about to the degrees of freedom of the two robotic arms. This part has been particularly laborious. For each robotic arm, we have imagined four possible solutions and for each of them CAD design is followed by the realization of a 3D mock-up. The final configuration was chosen in an attempt to reach a good compromise between a sufficiently robotic arms articulation (so as to allow surgical dissection) and the need for technical simplification to use the smallest possible number of motors, thereby reducing external dimensions. After a first attempt to assemble the 3D mock-up, it was decided to further simplify the gripper arm, exploiting slide movement by sliding out of the hood, thereby eliminating a motor.

The final prototype features are: gripper arm with pitch, sliding and open/close of the gripper; diathermic hook arm with pitch, roll and sliding of the entire arm. The degrees of freedom of the gripper arm are provided by three external motors located on the external box. The other arm is equipped with a diathermic hook and its movements (i.e., roll, pitch and sliding) are provided by three internal micro motors: two directly on the arm and one (to slide) into the hood. For the safety reason, one part of the gripper and the upper part of the RED

hood are coated with a plastic material (i.e., peek) to prevent accidental electrical discharges between diathermic hooks, gripper and the main body of the RED.

In summary, there will be 6 such distributed motors: 3 external motors for the gripper arms that will operate through cables contained in a sheath adherent to the colonoscope, and the internal motors for the diathermic hook arm.

Based on these technical specifications, 3D mock-ups of the individual parts in 1:1 scale (hood, gripper and diathermic hook arms) have been made, assembled and installed on the tip of an operative endoscope for to perform in-vitro test. The final purpose of this test was to evaluate the workspace and endoscopic field of view using a pelvic trainer for TEM. The test has shown that the operating field vision is not obstructed by the hood and the working range of the robot degrees of freedom is sufficiently wide to perform a dissection.

This final test concludes preliminary studies that have contributed to identify the overall layout of the RED: dimensions, degrees of freedom, number and distribution of engines needed for the operation of robotic arms; it is proved that the device, once assembled, maintained the visual and operational field characteristics necessary to perform an accurate dissection.

# **Chapter 6**

## **Conclusion**

CRC treatment is an important topic for Public Health. The implementation of screening programs and the use of colonoscopy has allowed the identification of an increasing number of early stage neoplastic lesions. The effectiveness of the treatment of rectal lesions with TEM technique contrasts to the technical limits of EMR and ESD techniques for the entire colon. The RED Robotic Platform aims to extend the accuracy of microsurgical dissection to the entire colon through the use of normal operating endoscopes, avoiding the purchase of expensive dedicated tools.

Tests conducted up to this point have allowed us to identify the overall layout of the RED: dimensions, degrees of freedom, number and distribution of motors needed for the operation of robotic arms; it also made it possible to verify that the device, once assembled, maintained the visual and operational field characteristics necessary to perform an accurate dissection.

The next step will be to realize a RED steel final prototype and in-vivo tests will be carry out to replicate an endoscopic dissection into the colon.

# References

- 1) Maida, M. (2017). Screening of colorectal cancer: present and future. *Expert Rev Anticancer Ther*, Epub ahead of print.
- 2) Xu, J. F. (2016). Endoscopic approach for superficial colorectal neoplasm. *Gastrointest Tumors*; 3(2):69-80.
- 3) Soetikno, R. M. (2003). Endoscopic mucosal resection. *Gastrointestinal endoscopy*, pages 567-579.
- 4) Gotoda, T. (2006). Endoscopic submucosal dissection for early gastric cancer. *Journal of Gastroenterology*, pages 929-942.
- 5) Kakushima, N. (2008). Endoscopic submucosal dissection for gastrointestinal neoplasm. *World J Gastroenterol*, pages 2962-2967.
- 6) Arezzo, A. (2014). Systematic review and meta-analysis of endoscopic submucosal dissection versus transanal endoscopic microsurgery for large noninvasive rectal lesions. *Surgical Endoscopy*, pages 427-438.
- 7) Morino, M. (2013). Transanal Endoscopic Microsurgery. *Techniques in coloproctology*, pages 55-61.
- 8) Vitiello, V. (2013). Emerging robotic platforms for minimally invasive surgery. *Biomedical Engineering, IEEE Reviews*, pages 111-126.
- 9) Obstein, K. L. (2013). Advanced endoscopic technologies for colorectal cancer screening. *World J Gastroenterol*, pages 431-439.
- 10) Karimyan, V. (2009). Navigation systems and platforms in natural orifice transluminal endoscopic surgery (NOTES). *International Journal of Surgery*, 297-304.



- 11) Yeung, B. P. M. (2012). A technical review of flexible endoscopic multitasking platforms. *International journal of surgery*, pages 345-354.
- 12) Phee, S. Y. (2012). Robot-assisted endoscopic submucosal dissection is effective in treating patients with early-stage gastric neoplasia. *Clinical Gastroenterology and Hepatology*, pages 1117-1121.
- 13) Phee, S. Y. (2009). Master and slave transluminal endoscopic robot (MASTER) for natural orifice transluminal endoscopic surgery (NOTES). *Engineering in Medicine and Biology Society. Annual International Conference of the IEEE. IEEE*, 2009.
- 14) Bardou, B. (2010). Design of a robotized flexible endoscope for natural orifice transluminal endoscopic surgery. *Computational Surgery and Dual Training. Springer US*, pages 155-170.
- 15) Bardou, B. (2009). Design of a telemanipulated system for transluminal surgery. *Engineering in Medicine and Biology Society. Annual International Conference of the IEEE. IEEE*, 2009.
- 16) Can, S. (2008). The mechatronic support system “HVSPS” and the way to NOTES. *Minimally invasive therapy & allied technologies*, pages 341-345.
- 17) Kobayashi, Y. (2010). A surgical robot with vision field control for single port endoscopic surgery. *The International Journal of Medical Robotics and Computer Assisted Surgery*, pages 454-464.
- 18) Shang, J. (2011). An articulated universal joint based flexible access robot for minimally invasive surgery. *Robotics and Automation (ICRA)*, 2011 IEEE International Conference.
- 19) Bajo, A. (2012). Integration and preliminary evaluation of an insertable robotic effectors platform for single port access surgery. *Robotics and Automation (ICRA)*, 2012 IEEE International Conference.

- 20) Shang, J. (2012). Design of a multitasking robotic platform with flexible arms and articulated head for minimally invasive surgery. *Intelligent Robots and Systems (IROS)*, 2012 IEEE/RSJ International Conference.
- 21) Lehman, A. C. (2011). Dexterous miniature robot for advanced minimally invasive surgery. *Surgical endoscopy*, pages 119-123.
- 22) Jayne, D. G. (2011). Robotic platforms for general and colorectal surgery. *Colorectal Disease*, pages 78-82.
- 23) Yeung, B. P. M. (2016). Application of robotics in gastrointestinal endoscopy: A review. *World journal of gastroenterology*, page 1811.
- 24) De Donno, A. (2013). Introducing STRAS: a new flexible robotic system for minimally invasive surgery. *Robotics and Automation (ICRA)*, 2013 IEEE International Conference.
- 25) Seneci, C. A. (2014). Design of a Bi-Manual End-Effector for an Endoscopic Surgical Robot. *The Hamlyn Symposium on Medical Robotics*.
- 26) Wortman, T. D. (2011). Laparoendoscopic single-site surgery using a multi-functional miniature in vivo robot. *The International Journal of Medical Robotics and Computer Assisted Surgery*, pages 17-21.
- 27) Dolghi, O. (2011). Miniature in vivo robot for laparoendoscopic single-site surgery. *Surgical endoscopy*, pages 3453-3458.
- 28) Shen, T. (2015). Design and Analysis of a Novel Articulated Drive Mechanism for Multifunctional NOTES Robot. *Journal of mechanisms and robotics*, pages 0110041-0110048.
- 29) Wortman, T. D. (2012). Miniature surgical robot for laparoendoscopic single-incision colectomy. *Surgical endoscopy*, pages 727-731.
- 30) Wortman, T. D. (2013). Single-site colectomy with miniature in vivo robotic platform. *Biomedical Engineering*, IEEE Transactions, pages 926-929.

- 31) Can, S. (2012). Design, development and evaluation of a highly versatile robot platform for minimally invasive single-port surgery. *Biomedical Robotics and Biomechatronics (BioRob)*, 2012 4th IEEE RAS & EMBS International Conference .
- 32) Kobayashi, Y. (2015). Development of a robotic system with six-degrees-of-freedom robotic tool manipulators for single-port surgery. *The International Journal of Medical Robotics and Computer Assisted Surgery*, pages 235-246.
- 33) Liu, Q. (2013). Development of a 6-DOF manipulator driven by flexible shaft for minimally invasive surgical application. *Engineering in Medicine and Biology Society (EMBC)*, 2013 35th Annual International Conference of the IEEE.
- 34) Petroni, G. (2013). A novel robotic system for single-port laparoscopic surgery: preliminary experience. *Surg Endosc*, 27(6) pages 1932-1937.
- 35) Phee, S. J. (2008). Robotic system for no-scar gastrointestinal surgery. *Int J Med Robot*, 4(1) pages 15-22.
- 36) Ranzani, T. (2015). A novel device for measuring forces in endoluminal procedures. *International Journal of Advances Robotic System*, 12:116 pages 1-10.
- 37) Alazmani, A. (2016). Quantitative assessment of colorectal morphology: implications for robotic colonoscopy. *Med Eng Phys*, 38(2) pages 148-154.